



**QUEEN'S
UNIVERSITY
BELFAST**

Secure Massive MIMO Relaying Systems in a Poisson Field of Eavesdroppers

Hoang, T. M., Duong, T. Q., Tuan, H. D., & Poor, H. V. (2017). Secure Massive MIMO Relaying Systems in a Poisson Field of Eavesdroppers. *IEEE Transactions on Communications*, 65(11).
<https://doi.org/10.1109/TCOMM.2017.2723565>

Published in:
IEEE Transactions on Communications

Document Version:
Peer reviewed version

Queen's University Belfast - Research Portal:
[Link to publication record in Queen's University Belfast Research Portal](#)

Publisher rights
© 2017 IEEE.

This work is made available online in accordance with the publisher's policies. Please refer to any applicable terms of use of the publisher.

General rights

Copyright for the publications made accessible via the Queen's University Belfast Research Portal is retained by the author(s) and / or other copyright owners and it is a condition of accessing these publications that users recognise and abide by the legal requirements associated with these rights.

Take down policy

The Research Portal is Queen's institutional repository that provides access to Queen's research output. Every effort has been made to ensure that content in the Research Portal does not infringe any person's rights, or applicable UK laws. If you discover content in the Research Portal that you believe breaches copyright or violates any law, please contact openaccess@qub.ac.uk.

Secure Massive MIMO Relaying Systems in a Poisson Field of Eavesdroppers

Tiep M. Hoang, *Student Member, IEEE*, Trung Q. Duong, *Senior Member, IEEE*, Hoang Duong Tuan, and H. Vincent Poor, *Fellow, IEEE*

Abstract—A cooperative relay network in the presence of eavesdroppers, whose locations are distributed according to a homogeneous Poisson point process, is considered. The relay is equipped with a very large antenna array and can exploit maximal ratio combining (MRC) in the uplink and maximal ratio transmission (MRT) in the downlink. We consider a realistic model that the channel state information of every eavesdropper is not known as eavesdroppers tend to hide themselves in practice. The destination is thus in a much weaker position than all the eavesdroppers because it only receives the retransmitted signal from the relay. Under such setting, we investigate the security performance in two schemes for relaying operation: amplify-and-forward (AF) and decode-and-forward (DF). The secrecy outage probability, the connection outage probability, and the trade-off problem which is controlled by the source power allocation are examined. Finally, suitable solutions for the source power (such that once the transmission occurs with high reliability, the secure risk is below a given threshold) are proposed for a trade-off between security and reliability issue.

Index terms—Security, massive MIMO, Poisson point process, maximum-ratio combining, maximum-ratio transmission, amplify-and-forward, decode-and-forward.

I. INTRODUCTION

Physical layer security (PLS) has attracted considerable attention from both academia and industry in recent years [1]. With the recent emergence of large antenna arrays [2], PLS is a promising approach for massive multiple-input multiple-output (MIMO) systems as countermeasures against eavesdropping attacks. Noticeably, the desired characteristics of massive MIMO systems are not present in conventional systems with small antenna arrays, e.g. an inner product of two random vectors can converge in distribution. Indeed, massive MIMO systems have been demonstrated to improve secure performance in several studies [3]–[12]. Having said

that, the role of massive MIMO systems in preventing eavesdroppers is not completely understood yet, mainly because PLS contains relatively many distinct aspects such as artificial noise (AN) technique, antenna/relay/jammer/user selection techniques, and strategies to deal with the leakage of information. Besides, different combinations of secure and relaying techniques also make security scenarios more diverse. Thus, the issue of security in massive MIMO relaying systems is still largely open.

Additionally, it should be mentioned that the assumption of presence of eavesdroppers is always of crucial importance. Several works assumed that the information of eavesdroppers is available at transmitters; however, that assumption is impractical in general. Since the location of eavesdroppers is typically not known, many authors have taken into account the spatial distribution of eavesdroppers by adopting a spatial point process model. For example, in order to model the spatial location of eavesdroppers, the authors in [13]–[15] used a homogeneous Poisson point process (PPP) model because of its mathematical tractability. It should also be noted that in the context of stochastic geometry, the PPP is the most widely used and important point process to describe spatially distributed discrete nodes [16]–[18]. Thus, the PPP will be adopted to model the spatial location of eavesdroppers in this paper.

Among recent works on the security for massive MIMO relaying systems [3]–[8], the authors in [3] and [4] considered cooperative relay systems and compared the security improvement for both amplify-and-forward (AF) and decode-and-forward (DF) relaying, while only the AF scheme (or the DF scheme) was considered in [5] and [6] (or in [7] and [8]). These works, however, did not consider any direct link between source and eavesdropper. Note that in general, eavesdroppers may possibly receive two versions of transmitted messages from source and relay in cooperative relay networks. The lack of direct links in [3]–[8] leads to the fact that the way eavesdroppers benefit from the configuration of cooperative relay networks is not sufficiently interpreted. Meanwhile, the impact of a direct eavesdropping link on the secure performance was presented in [19], but there was no discussion on large antenna arrays. Finally, other recent papers on secure massive MIMO networks (not necessarily relay-aided networks) can be also found out in the literature (e.g. [9]–[12]) with the discussion about the impact of the so-called *pilot contamination* scheme in which an eavesdropper can send a pilot sequence to attack massive MIMO systems,

T. M. Hoang and T. Q. Duong are with the School of Electronics, Electrical Engineering and Computer Science, The Queen's University of Belfast, Belfast BT7 1NN, Northern Ireland, The United Kingdom (e-mail: {mhoang02, trung.q.duong}@qub.ac.uk).

H. D. Tuan is with the Faculty of Engineering and Information Technology, University of Technology, Sydney, Australia (e-mail: tuan.hoang@uts.edu.au).

H. V. Poor is with the Department of Electrical Engineering, Princeton University, Princeton, NJ 08544 USA (e-mail: poor@princeton.edu).

This work was supported in part by the U.K. Royal Academy of Engineering Research Fellowship under Grant RF1415\14\22 and by the U.K. Engineering and Physical Sciences Research Council (EPSRC) under Grant EP/P019374/1, in part by the Australian Research Councils Discovery Projects under Project DP130104617, and in part by the U.S. National Science Foundation under Grants CMMI-1435778, ECCS-1549881 and ECCS-1647198. This paper was presented in part at the IEEE 85th Vehicular Technology Conference (VTC-Spring) in 2017.

but this context is beyond the scope of our paper.¹ Note that none of the above papers (i.e. [3]–[12]) discussed the spatial locations of eavesdroppers as a whole and the impact of direct eavesdropping links in particular.

On the contrary, the works in [13]–[15] considered the same assumption of the eavesdroppers' spatial distribution as in this work, but the topic of large antenna arrays was not discussed. For example, [13] analyzed the secure performance for millimeter wave systems instead of massive MIMO systems. While the authors in [14] and [15] used an artificial noise instead of large antenna arrays, to deal with eavesdropping attacks. Given that the artificial noise technique is also a signal generation process, it may be not necessarily adopted for large-scale antenna systems to reduce complexity, because such systems themselves can provide considerable benefits in terms of security [4]. Aiming to investigate the joint impact of massive MIMO systems and the eavesdroppers' geometric locations on the secure performance, [20] analyzed the secrecy outage probability (SOP) with emphasis on the possible areas of eavesdroppers. However, the geometric location of eavesdroppers in [20] is assumed to be uniformly distributed with a fixed number of eavesdroppers. Such an assumption is likely to be unreasonable for the wireless systems which do not have the knowledge of the number of stealthily working eavesdroppers. It is clear that the assumption of PPP has not yet adopted for secure massive MIMO systems as a whole, and secure massive MIMO relaying systems in particular.

In short, the works on security (mentioned in the above paragraphs) analyzed either massive MIMO system without the use of PPP, or conventional MIMO systems with the use of PPP. Thus, our work is to fill this gap by adopting the practical assumption of PPP for the cooperative wireless systems with large antenna arrays. In this paper, we consider a secure wireless network with the aid of a large antenna array at an intermediate relay. As for the relaying strategy at the relay, we choose to discuss conventional relaying schemes like the AF scheme and the DF scheme for comparison purposes, instead of delving into recently-developed relaying schemes (e.g. [21]). Around the relay, there exist many potential eavesdroppers whose location information is assumed to follow the PPP; thus, we take the direct links between source and eavesdroppers into account. While the direct link between source and destination is assumed to be impaired and neglected. Intuitively, all potential eavesdroppers are taking advantage of the physical setup model rather than the destination because they receive two versions of confidential signals. To elucidate how harmful the eavesdroppers can be, we evaluate the secure performance by using the SOP. Then we use an ON-OFF scheme for the transmission in which the source transmits its messages only when the legitimate channels are strong enough (i.e. reliable enough). To elucidate how reliable the secured transmission can be, we evaluate the performance by using the connection outage probability (COP). Finally, based on the SOP and the COP, we examine the most secured state at which our system is guaranteed at most, and show that this

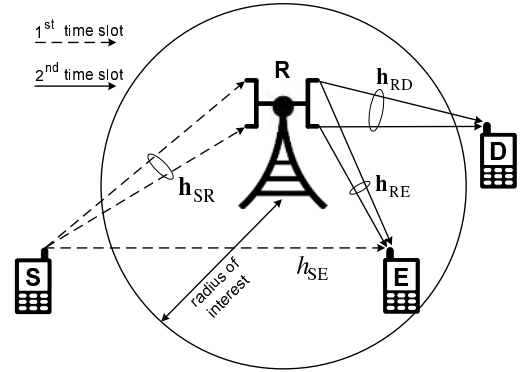


Fig. 1. System model.

state can be achieved when the source power is just slightly larger than a certain threshold (as long as the COP reaches 0). We also note that the asymptotic expressions are derived for the SOP and the COP in each distinct relaying strategy. We observe that if the ratio of the average transmit power at the source to the average noise power at the destination is high, the security aspect of the proposed system seems to depend on only the eavesdroppers' working range as well as the intensity of their presence. We also observe that when the source power increases, the SOP reaches its largest limit, while the COP equals 0. Besides, in both cases of relaying, the reliability of the system is demonstrated to gain from the increased number of antennas. Finally, our numerical results show the agreement between analysis and simulation.

The remainder of this paper is organized as follows: Section II describes the network configuration and restricts the case study to the worst case. In Section III, we provide the approximate characterization of the received signal-to-noise ratios (SNRs) under the influence of large antenna array. Sections IV and V derive the exact and asymptotic expressions for the SOP and the COP, respectively. In Section VI, two optimization problems are suggested for the AF scheme and the DF scheme to improve the secure performance. Numerical results are shown in Section VII and finally, conclusions are provided in Section VIII.

Notation: $[\cdot]^T$, $[\cdot]^*$, and $[\cdot]^\dagger$ denote the transpose operator, conjugate operator, and Hermitian operator, respectively. Vectors and matrices are represented with lowercase boldface and uppercase boldface, respectively. \mathbf{I}_n is the $n \times n$ identity matrix. $\|\cdot\|$ denotes the Euclidean norm. $\mathbb{E}\{\cdot\}$ denotes expectation. $\mathbf{z} \sim \mathcal{CN}_n(\mathbf{\Sigma})$ denotes a complex Gaussian vector $\mathbf{z} \in \mathbb{C}^{n \times 1}$ with zero-mean and covariance matrix $\mathbf{\Sigma} \in \mathbb{C}^{n \times n}$. $\text{Exp}(r)$ denotes the exponential distribution with rate r .

II. SYSTEM MODEL

As shown in Fig. 1, we consider a cooperative relay network in which there is a single source (S), a trusted relay (R), a destination (D), and multiple passive eavesdroppers (E_i with $i = 1, 2, \dots$).² The distance between S and D is very far so that

¹The context of pilot contamination can be ignored when considering a single cell, and especially when the pilot training only accounts for a very little portion of each coherence interval.

²We consider a practical scenario in which each E_i tends to hide itself, thus all eavesdroppers are referred to as passive.

R is invoked to help convey messages from S to D. As such, it is rational to consider that there is no direct link between S and D. However, the direct link between S and Ei is taken into account since Ei is likely to be present around S and/or R to overhear some confidential messages. We assume that R is equipped with a very large receive antenna array to decode its received signal in the uplink and a very large transmit antenna array to forward its decoded signal in the downlink; meanwhile, each of the remaining nodes (i.e. S, D and Ei) has only one antenna. It should be noted that both the number of transmit antennas and the number of receive antennas at R are equal to $N \gg 2$. The eavesdroppers are assumed to be spatially distributed according to a homogeneous PPP Ψ with intensity $\lambda > 0$, and yet they are only present within a circle $\mathcal{B}(R_\Psi R_0)$, which is centered at the origin R with the radius $R_\Psi R_0$.³ By keeping silent to steer clear of being detected, eavesdroppers do not get involved in actions like attacking pilot sequences.

Regarding propagation model, we discuss both small-scale and large-scale fading factors. The small-scale fading is characterized by $\mathbf{h}_{XY} \in \mathbb{C}^{n \times 1}$ (or $\mathbf{h}_{XY}^T \in \mathbb{C}^{n \times 1}$) with its signal magnitude being Rayleigh distributed. We assume that the column vector \mathbf{h}_{XY} (or \mathbf{h}_{XY}^T) obeys $\mathcal{CN}_n(\mathbf{I}_n)$. The large-scale fading is characterized by $l_{XY}^{-\alpha/2}$ with $\alpha > 2$ being the path-loss exponent and $l_{XY}R_0$ being the distance of the X–Y link. In path loss models [22]–[24], l_{XY} is understood as the ratio of the real distance to R_0 . For example, R_0 is often taken to be 100 m for microcells [24], then $l_{XY} = 2$ means that the real distance between X and Y is $2R_0 = 200$ m.

To facilitate the analysis, we use polar coordinates with R being the origin (as aforementioned) and ϕ being the angle $\widehat{\text{SRE}}i$. Then we have $l_{SE} = \sqrt{L_{SR}^2 + l^2 - 2L_{SR}l \cos \phi}$ with $L_{SR} \equiv l_{SR}$, $L_{RD} \equiv l_{RD}$ and $l \equiv l_{RE}$. Obviously, l_{SE} is a function of l and ϕ due to the random spatial distribution of Ei .

Regarding transmission, we use two equal time slots. In the first time slot, S transmits the source signal $s \in \mathbb{C}$ to R. In the second time slot, S keeps silent while R forwards the relaying signal $\mathbf{r} \in \mathbb{C}^{N \times 1}$ to D. In these two phases, both the signal transmitted from S (i.e. s) and the signal retransmitted from R (i.e. \mathbf{r}) are overheard by Ei .

- We normalize s such that $\mathbb{E}\{|s|^2\} = 1$, then the signals received at R and Ei in the first time slot are, respectively, written as

$$\mathbf{y}_R = \sqrt{\gamma_S} L_{SR}^{-\alpha/2} \mathbf{h}_{SR} s + \mathbf{n}_R, \quad (1)$$

$$y_{E,1} = \sqrt{\gamma_S} l_{SE}^{-\alpha/2} h_{SE} s + n_{E,1} \quad (2)$$

where $\mathbf{n}_R \sim \mathcal{CN}_N(\mathbf{I}_N)$ and $n_{E,1} \sim \mathcal{CN}_1(1)$ are the additive white Gaussian noises (AWGNs) at R and Ei , respectively; $L_{SR}^{-\alpha/2} \mathbf{h}_{SR} \in \mathbb{C}^{N \times 1}$ and $l_{SE}^{-\alpha/2} h_{SE} \in \mathbb{C}$ are the complex channel coefficients for the S-R and S- Ei links.

³It is of crucial important that if λ is measured by the average number of eavesdroppers over the area of R_0^2 , then average number of eavesdroppers within the circle $\mathcal{B}(R_\Psi R_0)$ is calculated as $\lambda \int_0^{R_\Psi} \int_0^{2\pi} l dl d\phi$ but not $\lambda \int_0^{R_\Psi R_0} \int_0^{2\pi} l dl d\phi$. Herein, R_0 is referred to as a reference distance, while R_Ψ is the ratio of the real radius to R_0 . For example, if we have $R_0 = 1$ km and $R_\Psi = 2$, the radius of the considered circle will be 2 km.

- We normalize \mathbf{r} such that $\mathbb{E}\{\mathbf{r}\mathbf{r}^\dagger\} = \mathbf{I}_N$, then the signals received at D and Ei in the second time slot are, respectively, written as

$$y_D = \sqrt{\gamma_R/N} L_{RD}^{-\alpha/2} \mathbf{h}_{RD}^T \mathbf{r} + n_D, \quad (3)$$

$$y_{E,2} = \sqrt{\gamma_R/N} l_{RE}^{-\alpha/2} \mathbf{h}_{RE}^T \mathbf{r} + n_{E,2} \quad (4)$$

where $n_D \sim \mathcal{CN}_1(1)$ and $n_{E,2} \sim \mathcal{CN}_1(1)$ are AWGNs at D and Ei , respectively; $L_{RD}^{-\alpha/2} \mathbf{h}_{RD} \in \mathbb{C}^{1 \times N}$ and $l_{RE}^{-\alpha/2} \mathbf{h}_{RE} \in \mathbb{C}^{1 \times N}$ are the complex channel coefficients the R-D and R- Ei links.

We note that for simplification purpose, the average noise power at each receive antenna is assumed to be the same. This leads to the fact that both (1) and (2) contain the same γ_S , while both (3) and (4) contain the same γ_R . With the noise normalization, γ_S is both the average received SNR per antenna at R and the average received SNR at Ei , while γ_R is the average received SNR at D as well as Ei . It should also be noted that the subscript $[\cdot]_E$ is implicitly related to Ei with $i \in \Psi$; however, the index i is dropped for notational simplicity.

A. MRC/MRT at Relay

After being received at R, the signal \mathbf{y}_R is then multiplied by a weighting vector $\mathbf{w}^\dagger \in \mathbb{C}^{1 \times N}$ through a process called MRC to combine N received signals in (1). Moreover, in the uplink, \mathbf{w} is designed only based on \mathbf{h}_{SR} because the instantaneous h_{SE} is not known (i.e. there is no the CSI of Ei).⁴ Hence, according to MRC principle, we have $\mathbf{w} = \mathbf{h}_{SR}/\|\mathbf{h}_{SR}\|$. The obtained signal after this process can be written as

$$r_0 = \mathbf{w}^\dagger \mathbf{y}_R = \sqrt{\gamma_S} L_{SR}^{-\alpha/2} \|\mathbf{h}_{SR}\| s + \frac{\mathbf{h}_{SR}^\dagger}{\|\mathbf{h}_{SR}\|} \mathbf{n}_R. \quad (5)$$

The MRC output signal r_0 is then processed by R according to relaying operation (AF scheme or DF scheme). Consequently, the obtained signal posterior to relaying operation is \widehat{r}_0 which is then multiplied by another weighting vector $\mathbf{v} \in \mathbb{C}^{N \times 1}$ to form the retransmitted signal \mathbf{r} . In the same way as the design of \mathbf{w} , the weighting vector \mathbf{v} is designed only based on \mathbf{h}_{RD} . As such, applying MRT to the downlink, we have $\mathbf{v} = \mathbf{h}_{RD}^*/\|\mathbf{h}_{RD}\|$. Hence, the relation between the decoded signal \widehat{r}_0 and the retransmitted signal \mathbf{r} can be given by

$$\mathbf{r} = \mathbf{v} \widehat{r}_0 = \frac{\mathbf{h}_{RD}^*}{\|\mathbf{h}_{RD}\|} \widehat{r}_0. \quad (6)$$

In the following, the expressions for \widehat{r}_0 will be discussed based on two different relaying operations, namely, AF scheme and DF scheme.

1) *AF Scheme at R*: In this case, the signal \widehat{r}_0 is simply a scaled version of the signal r_0 , i.e.

$$\widehat{r}_0 = c^{AF} r_0 \quad (7)$$

where c^{AF} is a constant subject to the following transmit power constraint

$$\text{tr}(\mathbb{E}\{\mathbf{r}\mathbf{r}^\dagger\}) = \text{tr}(\mathbf{I}_N) = N. \quad (8)$$

⁴Since the design of \mathbf{w} does not take h_{SE} into account due to the lack of the CSI of Ei , the design of \mathbf{w} according to MRC principle is not the optimal solution in terms of security.

Using (5)–(8) yields

$$c^{AF} = \sqrt{\frac{N}{\gamma_S L_{SR}^{-\alpha} \|\mathbf{h}_{SR}\|^2 + 1}}. \quad (9)$$

Substituting (5) and (9) into (6)–(7), we obtain a new expression of \mathbf{r} and then again substituting this new expression into (3)–(4), we can rewrite (3)–(4) as

$$y_D^{AF} = \sqrt{\frac{\gamma_S \gamma_R L_{SR}^{-\alpha} L_{RD}^{-\alpha} \|\mathbf{h}_{SR}\|^2}{\gamma_S L_{SR}^{-\alpha} \|\mathbf{h}_{SR}\|^2 + 1}} \|\mathbf{h}_{RD}\| s + n_D^{AF}, \quad (10)$$

$$y_{E,2}^{AF} = \sqrt{\frac{\gamma_S \gamma_R L_{SR}^{-\alpha} l^{-\alpha} \|\mathbf{h}_{SR}\|^2}{\gamma_S L_{SR}^{-\alpha} \|\mathbf{h}_{SR}\|^2 + 1}} \frac{\mathbf{h}_{RE}^T \mathbf{h}_{RD}^*}{\|\mathbf{h}_{RD}\|} s + n_{E,2}^{AF} \quad (11)$$

where

$$n_D^{AF} \triangleq \sqrt{\frac{\gamma_R L_{RD}^{-\alpha} \|\mathbf{h}_{RD}\|^2}{\gamma_S L_{SR}^{-\alpha} \|\mathbf{h}_{SR}\|^2 + 1}} \frac{\mathbf{h}_{SR}^\dagger}{\|\mathbf{h}_{SR}\|} \mathbf{n}_R + n_D, \quad (12)$$

$$n_{E,2}^{AF} \triangleq \sqrt{\frac{\gamma_R l^{-\alpha}}{\gamma_S L_{SR}^{-\alpha} \|\mathbf{h}_{SR}\|^2 + 1}} \frac{\mathbf{h}_{RE}^T \mathbf{h}_{RD}^* \mathbf{h}_{SR}^\dagger}{\|\mathbf{h}_{RD}\| \|\mathbf{h}_{SR}\|} \mathbf{n}_R + n_{E,2}. \quad (13)$$

2) *DF Scheme at R*: In this case, we consider the case that both the source and the relay use the same codeword for their transmission [25]. The signal \hat{r}_0 is successfully decoded from the signal r_0 , thus we have the following relation

$$\hat{r}_0 = c^{DF} s, \quad (14)$$

where c^{DF} is a constant subject to the constraint (8). From (6), (8) and (14), we have $c^{DF} = \sqrt{N}$ whereby (6) can be given by

$$\mathbf{r} = \frac{\mathbf{h}_{RD}^*}{\|\mathbf{h}_{RD}\|} \sqrt{N} s. \quad (15)$$

Substituting the above expression into (3)–(4), we can rewrite (3)–(4) as

$$y_D^{DF} = \sqrt{\gamma_R} L_{RD}^{-\alpha/2} \|\mathbf{h}_{RD}\| s + n_D, \quad (16)$$

$$y_{E,2}^{DF} = \sqrt{\gamma_R} l^{-\alpha/2} \frac{\mathbf{h}_{RE}^T \mathbf{h}_{RD}^*}{\|\mathbf{h}_{RD}\|} s + n_{E,2}. \quad (17)$$

B. Signal-to-Noise Ratios in the Worst Case

A wise E_i can be capable of exploiting the best possible decoding strategy to maximize its received signals. Herein, we suppose that E_i is able to use MRC process to combine one signal from S and N signals from R. Obviously, the strategy of malicious eavesdroppers in AF scheme is different from that in DF scheme.

1) *AF Scheme at R*: From (2) and (11), the overall received signals at E_i can be written as

$$\mathbf{y}_E^{AF} = \underbrace{\left[\sqrt{\frac{\gamma_S \gamma_R L_{SR}^{-\alpha} l^{-\alpha} \|\mathbf{h}_{SR}\|^2}{\gamma_S L_{SR}^{-\alpha} \|\mathbf{h}_{SR}\|^2 + 1}} \frac{\mathbf{h}_{RE}^T \mathbf{h}_{RD}^*}{\|\mathbf{h}_{RD}\|} \right]}_{\triangleq \mathbf{g}^{AF}} s + \underbrace{\begin{bmatrix} n_{E,1} \\ n_{E,2} \end{bmatrix}}_{\triangleq \tilde{\mathbf{n}}^{AF}}. \quad (18)$$

Then using MRC receiver with the weighting vector \mathbf{f}^{AF} , we can write the combined output at E_i as

$$z_E^{AF} = (\mathbf{f}^{AF})^\dagger \mathbf{g}^{AF} s + (\mathbf{f}^{AF})^\dagger \tilde{\mathbf{n}}^{AF}. \quad (19)$$

From (19), the instantaneous SNR at E_i can be generally written as [26]⁵

$$\widehat{\text{SNR}}_E(\mathbf{f}^{AF}) = \frac{(\mathbf{f}^{AF})^\dagger (\mathbf{g}^{AF} (\mathbf{g}^{AF})^\dagger) \mathbf{f}^{AF}}{(\mathbf{f}^{AF})^\dagger \tilde{\mathbf{R}}^{AF} \mathbf{f}^{AF}} \leq (\mathbf{g}^{AF})^\dagger (\tilde{\mathbf{R}}^{AF})^{-1} \mathbf{g}^{AF} \quad (20)$$

where $\tilde{\mathbf{R}}^{AF}$ is the covariance matrix of $\tilde{\mathbf{n}}^{AF}$. The equality in (20) holds for

$$\mathbf{f}^{AF} = \tau (\tilde{\mathbf{R}}^{AF})^{-1} \mathbf{g}^{AF} \triangleq \mathbf{f}_{opt}^{AF} \quad (21)$$

with τ being an arbitrary constant. It is apparent that in practice, a wise E_i is likely to design $\mathbf{f}^{AF} = \mathbf{f}_{opt}^{AF}$ to maximize its received SNR. Taking this into account, we assume that the received SNR at E_i is

$$\widehat{\text{SNR}}_E \equiv \widehat{\text{SNR}}_E(\mathbf{f}_{opt}^{AF}) = (\mathbf{g}^{AF})^\dagger (\tilde{\mathbf{R}}^{AF})^{-1} \mathbf{g}^{AF}. \quad (22)$$

As such, we will only discuss this practical scenario throughout the rest of this paper.

The covariance matrix of $\tilde{\mathbf{n}}^{AF}$ in (18) can be expressed as

$$\begin{aligned} \tilde{\mathbf{R}}^{AF} &= \mathbb{E} \left\{ \tilde{\mathbf{n}}^{AF} (\tilde{\mathbf{n}}^{AF})^\dagger \right\} \\ &= \begin{bmatrix} 1 & 0 \\ 0 & \frac{\gamma_R l^{-\alpha} |\mathbf{h}_{RE}^T \mathbf{h}_{RD}^*|^2}{(\gamma_S L_{SR}^{-\alpha} \|\mathbf{h}_{SR}\|^2 + 1) \|\mathbf{h}_{RD}\|^2} + 1 \end{bmatrix}. \end{aligned} \quad (23)$$

Substituting \mathbf{g}^{AF} in (18) and $\tilde{\mathbf{R}}^{AF}$ in (23) into (22), we can write the instantaneous SNR at E_i in the case of AF as

$$\widehat{\text{SNR}}_E^{AF} = \frac{\gamma_S L_{SR}^{-\alpha} \gamma_R l^{-\alpha} \|\mathbf{h}_{SR}\|^2 |\mathbf{h}_{RD}^T \mathbf{h}_{RE}^*|^2}{(\gamma_S L_{SR}^{-\alpha} \|\mathbf{h}_{SR}\|^2 + 1) \|\mathbf{h}_{RD}\|^2 + \gamma_R l^{-\alpha} |\mathbf{h}_{RD}^T \mathbf{h}_{RE}^*|^2 + \gamma_S l_{SE}^{-\alpha} |h_{SE}|^2}. \quad (24)$$

From (10), the instantaneous SNR at D can be given by

$$\widehat{\text{SNR}}_D^{AF} = \frac{\gamma_S L_{SR}^{-\alpha} \gamma_R L_{RD}^{-\alpha} \|\mathbf{h}_{SR}\|^2 \|\mathbf{h}_{RD}\|^2}{\gamma_S L_{SR}^{-\alpha} \|\mathbf{h}_{SR}\|^2 + \gamma_R L_{RD}^{-\alpha} \|\mathbf{h}_{RD}\|^2 + 1}. \quad (25)$$

2) *DF Scheme at R*: Unlike the AF scheme, the expressions of SNRs for the DF scheme are formulated in a different way. When only considering the indirect transmission from S to D through R, we can infer the instantaneous SNR at E_i from (1) and (17) as follows [29]:

$$\widehat{\text{SNR}}_{E, \text{indirect}}^{DF} = \min \left\{ \gamma_S L_{SR}^{-\alpha} \|\mathbf{h}_{SR}\|^2, \gamma_R l^{-\alpha} \frac{|\mathbf{h}_{RD}^T \mathbf{h}_{RE}^*|^2}{\|\mathbf{h}_{RD}\|^2} \right\}. \quad (26)$$

⁵Since the term $\tilde{\mathbf{R}}^{AF}$ in (20) is positive definite, we can factorize it into $\mathbf{U}^\dagger \mathbf{U}$ by using Cholesky decomposition. The left hand side of (20) can be rewritten as $\widehat{\text{SNR}}_E(\mathbf{f}_0) = \left[\mathbf{f}_0^\dagger (\mathbf{g}_0 \mathbf{g}_0^\dagger) \mathbf{f}_0 \right] / \left(\mathbf{f}_0^\dagger \mathbf{f}_0 \right)$ where $\mathbf{f}_0 \triangleq \mathbf{U} \mathbf{f}^{AF} \in \mathbb{C}^{2 \times 1}$ and $\mathbf{g}_0 \triangleq (\mathbf{U}^\dagger)^{-1} \mathbf{g}^{AF} \in \mathbb{C}^{2 \times 1}$. Obviously, the new expression of the instantaneous SNR at E_i with respect to \mathbf{f}_0 is now a Rayleigh quotient [27]–[28], therefore we have $\max_{\mathbf{f}_0} \widehat{\text{SNR}}_E(\mathbf{f}_0) = \lambda_{\max}(\mathbf{g}_0 \mathbf{g}_0^\dagger) = \|\mathbf{g}_0\|^2$ where λ_{\max} is the maximum eigenvalue of $\mathbf{g}_0 \mathbf{g}_0^\dagger$, and the last equality follows from that $\mathbf{g}_0 \mathbf{g}_0^\dagger$ is of one rank. Then the right hand side of (20) is obtained by substituting $\mathbf{g}_0 = (\mathbf{U}^\dagger)^{-1} \mathbf{g}^{AF}$ and $\mathbf{U}^\dagger \mathbf{U} = \tilde{\mathbf{R}}^{AF}$.

Similarly, when only considering the direct S-Ei link, we can infer the instantaneous SNR at Ei from (2), i.e.

$$\widehat{\text{SNR}}_{E, \text{direct}}^{DF} = \gamma_S l_{SE}^{-\alpha} |h_{SE}|^2. \quad (27)$$

Finally, with the assumption that Ei uses MRC technique to combine signals from direct and indirect links, the instantaneous SNR at Ei can be given by [26]:

$$\begin{aligned} \widehat{\text{SNR}}_E^{DF} &= \widehat{\text{SNR}}_{E, \text{indirect}}^{DF} + \widehat{\text{SNR}}_{E, \text{direct}}^{DF} \\ &= \min \left\{ \gamma_S L_{SR}^{-\alpha} \|\mathbf{h}_{SR}\|^2, \gamma_R l^{-\alpha} \frac{|\mathbf{h}_{RD}^T \mathbf{h}_{RE}^*|^2}{\|\mathbf{h}_{RD}\|^2} \right\} + \gamma_S l_{SE}^{-\alpha} |h_{SE}|^2. \end{aligned} \quad (28)$$

From (1) and (16), the instantaneous SNR at D can be given by [29]

$$\widehat{\text{SNR}}_D^{DF} = \min \left\{ \gamma_S L_{SR}^{-\alpha} \|\mathbf{h}_{SR}\|^2, \gamma_R L_{RD}^{-\alpha} \|\mathbf{h}_{RD}\|^2 \right\}. \quad (29)$$

Observation: From (24)–(25) we can see that both $\widehat{\text{SNR}}_E^{AF}$ and $\widehat{\text{SNR}}_D^{DF}$ are increasing functions of γ_S . Thus, there will be a need to find out a suitable value of γ_S in making the trade-off between these SNRs. In contrast, the same does not hold for $\widehat{\text{SNR}}_E^{DF}$ and $\widehat{\text{SNR}}_D^{DF}$. In both relaying operations, γ_R will not be examined for our trade-off problem. With the large number of antennas configured at R, it is plausible to remain the average total relay power (i.e. γ_R) constant such that the consumed power per-antenna unit at R is reduced.

III. THE SNR APPROXIMATION UNDER THE IMPACT OF LARGE ANTENNA ARRAYS

In this section, we will evaluate the secure performance of the proposed system under the assumption that the number of transmit and receive antennas at R is very large. Recall the following well-known properties:⁶

- Property (P1): Let $\mathbf{p} \in \mathbb{C}^{N \times 1}$ and $\mathbf{q} \in \mathbb{C}^{N \times 1}$ be complex-valued column vectors whose elements are i.i.d. random variables with zero mean and variances of σ_p^2 and σ_q^2 . Then $(1/\sqrt{N})\mathbf{p}^T \mathbf{q} \xrightarrow{\text{dist}} \mathcal{CN}(0, \sigma_p^2 \sigma_q^2)$ where $\xrightarrow{\text{dist}}$ denotes convergence in distribution as $N \rightarrow \infty$.
- Property (P2): With \mathbf{p} and \mathbf{q} as in (P1), we have $\frac{1}{N} \|\mathbf{p}\|^2 \xrightarrow{N \rightarrow \infty} \sigma_p^2$ as well as $\frac{1}{N} \|\mathbf{q}\|^2 \xrightarrow{N \rightarrow \infty} \sigma_q^2$ where $\xrightarrow{N \rightarrow \infty}$ denotes convergence as $N \rightarrow \infty$.

To proceed, we first rewrite (24)–(25) as

$$\widehat{\text{SNR}}_D^{AF} = N \frac{\gamma_S L_{SR}^{-\alpha} \gamma_R L_{RD}^{-\alpha} \frac{\|\mathbf{h}_{SR}\|^2 \|\mathbf{h}_{RD}\|^2}{N}}{\gamma_S L_{SR}^{-\alpha} \frac{\|\mathbf{h}_{SR}\|^2}{N} + \gamma_R L_{RD}^{-\alpha} \frac{\|\mathbf{h}_{RD}\|^2}{N} + \frac{1}{N}}, \quad (30)$$

$$\begin{aligned} \widehat{\text{SNR}}_E^{AF} &= \gamma_S l_{SE}^{-\alpha} |h_{SE}|^2 \\ &+ N \frac{\gamma_S L_{SR}^{-\alpha} \gamma_R l^{-\alpha} \frac{\|\mathbf{h}_{SR}\|^2 \|\mathbf{h}_{RD}^T \mathbf{h}_{RE}^*\|^2}{N}}{N \left(\gamma_S L_{SR}^{-\alpha} \frac{\|\mathbf{h}_{SR}\|^2}{N} + \frac{1}{N} \right) \frac{\|\mathbf{h}_{RD}\|^2}{N} + \gamma_R l^{-\alpha} \frac{\|\mathbf{h}_{RD}^T \mathbf{h}_{RE}^*\|^2}{N}} \end{aligned} \quad (31)$$

⁶These properties are derived from the Lindeberg-Levy theorem and law of large numbers (see [2], [30], [31] and references therein).

and (28)–(29) as

$$\widehat{\text{SNR}}_D^{DF} = N \min \left\{ \gamma_S L_{SR}^{-\alpha} \frac{\|\mathbf{h}_{SR}\|^2}{N}, \gamma_R L_{RD}^{-\alpha} \frac{\|\mathbf{h}_{RD}\|^2}{N} \right\}, \quad (32)$$

$$\begin{aligned} \widehat{\text{SNR}}_E^{DF} &= \gamma_S l_{SE}^{-\alpha} |h_{SE}|^2 \\ &+ N \min \left\{ \gamma_S L_{SR}^{-\alpha} \frac{\|\mathbf{h}_{SR}\|^2}{N}, \gamma_R l^{-\alpha} \frac{|\mathbf{h}_{RD}^T \mathbf{h}_{RE}^*|^2}{N} \frac{\frac{1}{N}}{\frac{\|\mathbf{h}_{RD}\|^2}{N}} \right\}. \end{aligned} \quad (33)$$

Then, respectively applying Property (P1) to the term $\frac{\mathbf{h}_{RD}^T \mathbf{h}_{RE}^*}{\sqrt{N}}$ and applying Property (P2) to the terms $\frac{\|\mathbf{h}_{SR}\|^2}{N}$ and $\frac{\|\mathbf{h}_{RD}\|^2}{N}$, we can arrive at the following approximate expressions:

$$\widehat{\text{SNR}}_D^{AF} \xrightarrow{N \rightarrow \infty} \frac{\gamma_S L_{SR}^{-\alpha} \gamma_R L_{RD}^{-\alpha} N^2}{\gamma_S L_{SR}^{-\alpha} N + \gamma_R L_{RD}^{-\alpha} N + 1} \triangleq \text{snr}_D^{AF}, \quad (34)$$

$$\begin{aligned} \widehat{\text{SNR}}_E^{AF} &\xrightarrow{N \rightarrow \infty} \frac{\gamma_S L_{SR}^{-\alpha} \gamma_R l^{-\alpha} N \Theta}{(\gamma_S L_{SR}^{-\alpha} N + 1) + \gamma_R l^{-\alpha} \Theta} + \gamma_S l_{SE}^{-\alpha} |h_{SE}|^2 \\ &\triangleq \text{snr}_E^{AF}, \end{aligned} \quad (35)$$

$$\widehat{\text{SNR}}_D^{DF} \xrightarrow{N \rightarrow \infty} \min \left\{ \gamma_S L_{SR}^{-\alpha} N, \gamma_R L_{RD}^{-\alpha} N \right\} \triangleq \text{snr}_D^{DF}, \quad (36)$$

$$\begin{aligned} \widehat{\text{SNR}}_E^{DF} &\xrightarrow{N \rightarrow \infty} \min \left\{ \gamma_S L_{SR}^{-\alpha} N, \gamma_R l^{-\alpha} \Theta \right\} + \gamma_S l_{SE}^{-\alpha} |h_{SE}|^2 \\ &\triangleq \text{snr}_E^{DF} \end{aligned} \quad (37)$$

where $\Theta \triangleq \frac{1}{N} \left| \mathbf{h}_{RD} \mathbf{h}_{RE}^\dagger \right|^2$. Note that we have $\frac{1}{\sqrt{N}} \mathbf{h}_{RD} \mathbf{h}_{RE}^\dagger \xrightarrow{\text{dist}} \mathcal{CN}(0, 1)$ by using Property (P1) and thus, $\Theta \sim \text{Exp}(1)$.⁷ In (34)–(37), snr_D^{AF} , snr_E^{AF} , snr_D^{DF} and snr_E^{DF} are defined as functions in N .

Let E_{max} denote the strongest eavesdropper that is receiving the largest instantaneous SNR among all eavesdroppers $E_i \in \Psi$. Then the instantaneous SNRs at E_{max} in the AF scheme ($\widehat{\text{SNR}}_{E_{max}}^{AF}$) and in the DF scheme ($\widehat{\text{SNR}}_{E_{max}}^{DF}$) are approximated as

$$\widehat{\text{SNR}}_{E_{max}}^{AF} \equiv \max_{E_i \in \Psi} \widehat{\text{SNR}}_E^{AF} \xrightarrow{N \rightarrow \infty} \max_{E_i \in \Psi} \text{snr}_E^{AF}, \quad (38)$$

$$\widehat{\text{SNR}}_{E_{max}}^{DF} \equiv \max_{E_i \in \Psi} \widehat{\text{SNR}}_E^{DF} \xrightarrow{N \rightarrow \infty} \max_{E_i \in \Psi} \text{snr}_E^{DF}. \quad (39)$$

To facilitate the general analysis which can be applied to both schemes, we use the following notations: $\widehat{\text{SNR}}_D = \left\{ \widehat{\text{SNR}}_D^{AF}, \widehat{\text{SNR}}_D^{DF} \right\}$, $\widehat{\text{SNR}}_E = \left\{ \widehat{\text{SNR}}_E^{AF}, \widehat{\text{SNR}}_E^{DF} \right\}$, $\text{snr}_D = \left\{ \text{snr}_D^{AF}, \text{snr}_D^{DF} \right\}$, $\text{snr}_E = \left\{ \text{snr}_E^{AF}, \text{snr}_E^{DF} \right\}$, and $\max_{E_i \in \Psi} \text{snr}_E = \left\{ \max_{E_i \in \Psi} \text{snr}_E^{AF}, \max_{E_i \in \Psi} \text{snr}_E^{DF} \right\}$.

Proposition 1. *The cumulative distribution function (CDF) of snr_E^{AF} is given by*

$$\begin{aligned} F_{\text{snr}_E^{AF}}(\mu) &= 1 - \mathcal{T}_{\mu_m}(l) \mathbb{1}(\mu_m < \gamma_S L_{SR}^{-\alpha} N) \\ &\quad - \frac{\gamma_S L_{SR}^{-\alpha} N (1 + \gamma_S L_{SR}^{-\alpha} N)}{\gamma_R l^{-\alpha}} \mathcal{J}_{\mu_m}(l, l_{SE}) \end{aligned} \quad (40)$$

where

$$\mu_m \triangleq \min \{ \mu, \gamma_S L_{SR}^{-\alpha} N \},$$

⁷ $\text{Exp}(r)$ denotes the exponential distribution with rate r . If $z \sim \mathcal{CN}(0, \sigma^2)$, then $|z|^2 \sim \text{Exp}(1/\sigma^2)$.

$$\mathbb{1}(\mathbf{C}) = \begin{cases} 1, & \text{if } \mathbf{C} \text{ is true} \\ 0, & \text{otherwise} \end{cases}, \quad (41)$$

$$\mathcal{T}_{\mu_m}(l) \triangleq \exp \left\{ \frac{(1 + \gamma_S L_{SR}^{-\alpha} N) \mu_m}{\gamma_R l^{-\alpha} (\mu_m - \gamma_S L_{SR}^{-\alpha} N)} \right\} \quad (42)$$

and

$$\mathcal{J}_{\mu_m}(l, l_{SE}) \triangleq e^{-\frac{\mu}{\gamma_S l_{SE}^{-\alpha}}} \int_0^{\mu_m} \frac{e^{\frac{x}{\gamma_S l_{SE}^{-\alpha}} + \frac{(1 + \gamma_S L_{SR}^{-\alpha} N)x}{\gamma_R l^{-\alpha} (x - \gamma_S L_{SR}^{-\alpha} N)}}}{(x - \gamma_S L_{SR}^{-\alpha} N)^2} dx. \quad (43)$$

Proof. See Appendix A. \square

Proposition 2. The CDF of snr_E^{DF} is given by

$$\begin{aligned} F_{\text{snr}_E^{DF}}(\mu) &= 1 - e^{-\frac{\mu_m}{\gamma_R l^{-\alpha}}} \\ &+ \frac{\gamma_S l_{SE}^{-\alpha}}{\gamma_R l^{-\alpha} - \gamma_S l_{SE}^{-\alpha}} e^{-\frac{\mu}{\gamma_S l_{SE}^{-\alpha}}} \left[1 - e^{\mu_m \left(\frac{1}{\gamma_S l_{SE}^{-\alpha}} - \frac{1}{\gamma_R l^{-\alpha}} \right)} \right] \\ &+ e^{-\frac{\gamma_S L_{SR}^{-\alpha} N}{\gamma_R l^{-\alpha}}} \left[1 - e^{-\frac{(\mu - \mu_m)}{\gamma_S l_{SE}^{-\alpha}}} \right] \mathbb{1}(\mu > \gamma_S L_{SR}^{-\alpha} N). \end{aligned} \quad (44)$$

Proof. See Appendix B. \square

IV. SECRECY OUTAGE PROBABILITY (SOP)

In this section, we evaluate the secure performance of the proposed system through the SOP. We first suppose that each E_i succeeds in partially decoding the received signal if its instantaneous SNR is large than or equal to a certain threshold μ at the receiver of E_i . When eavesdroppers are non-colluding, we can define an *outage event* as the event in which “there is at least a certain E_i which can partially decode its received signal.” Based on this definition, the SOP is referred to as the probability of the occurrence of the *outage event*, i.e.

$$\begin{aligned} \widehat{\text{SOP}}_{\mu} &\triangleq \mathbb{P} \{ \text{outage event} \} \\ &= \mathbb{P} \left\{ \exists E_i \in \Psi \mid \widehat{\text{SNR}}_E \geq \mu \right\} \\ &= \mathbb{P} \left\{ \max_{E_i \in \Psi} \widehat{\text{SNR}}_E \geq \mu \right\} \end{aligned} \quad (45)$$

in which $\max_{E_i \in \Psi} \widehat{\text{SNR}}_E \geq \mu$ implies that among existing eavesdroppers, the eavesdropper with the maximum received SNR can decode signals.⁸

A. Analysis with large N

Under the assumption of (very) large N , we can use (45), (38) and (39) to arrive at the following approximation

$$\begin{aligned} \widehat{\text{SOP}}_{\mu} &\xrightarrow{N \rightarrow \infty} \text{SOP}_{\mu} = \mathbb{P} \left\{ \max_{E_i \in \Psi} \text{snr}_E \geq \mu \right\} \\ &= 1 - \mathbb{E}_{\Psi} \left\{ \prod_{E_i \in \Psi} \mathbb{P} \{ \text{snr}_E < \mu \mid \Psi \} \right\} \\ &\stackrel{(a)}{=} 1 - \exp \left\{ -\lambda \int_0^{2\pi} \int_0^{R_{\Psi}} (1 - F_{\text{snr}_E}(\mu)) l dl d\phi \right\} \end{aligned} \quad (46)$$

⁸For the colluding eavesdroppers scenario, the outage event should be defined as the event of the occurrence $\sum_{E_i \in \Psi} \widehat{\text{SNR}}_E \geq \mu$. This interesting scenario might not be mathematically tractable and will be considered in the future.

where the equality (a) follows from the *probability generating functional* (PGF) [16]. Herein, $\mathbb{P} \{ \text{snr}_E < \mu \mid \Psi \} = F_{\text{snr}_E}(\mu)$ is the probability that a certain E_i cannot decode the received signal. In the following, we evaluate the SOP for two schemes of interest. Note that $\text{SOP}_{\mu} \equiv \text{SOP}_{\mu}^{AF}$ and $\text{SOP}_{\mu} \equiv \text{SOP}_{\mu}^{DF}$ for the two different relaying cases.

1) *AF scheme:* The SOP in the AF case is given by

$$\text{SOP}_{\mu}^{AF} = 1 - \exp \left\{ -\lambda \int_0^{2\pi} \int_0^{R_{\Psi}} \underbrace{(1 - F_{\text{snr}_E^{AF}}(\mu))}_{\text{a function of } l \text{ and } \phi} l dl d\phi \right\}. \quad (47)$$

By substituting (40) into (47), we have

$$\begin{aligned} \text{SOP}_{\mu}^{AF} &= 1 - \exp \left\{ -\lambda \int_0^{2\pi} \int_0^{R_{\Psi}} \left[\mathcal{T}_{\mu_m}(l) \mathbb{1}(\mu_m < \gamma_S L_{SR}^{-\alpha} N) \right. \right. \\ &\quad \left. \left. + \frac{\gamma_S L_{SR}^{-\alpha} N (1 + \gamma_S L_{SR}^{-\alpha} N)}{\gamma_R l^{-\alpha}} \mathcal{J}_{\mu_m}(l, l_{SE}) \right] l dl d\phi \right\} \end{aligned} \quad (48)$$

which can also be explicitly presented as in (49) at the top of the next page.

2) *DF scheme:* The SOP in the DF case is given by

$$\text{SOP}_{\mu}^{DF} = 1 - \exp \left\{ -\lambda \int_0^{2\pi} \int_0^{R_{\Psi}} \underbrace{(1 - F_{\text{snr}_E^{DF}}(\mu))}_{\text{a function of } l \text{ and } \phi} l dl d\phi \right\} \quad (50)$$

by repeating the same steps as in the derivation of (47). Substituting (44) into the above equation, we arrive at the final exact expression for (50) as shown in (55) at the top of the next page.

B. Analysis with large N and high γ_S

With very large N , we proceed to consider the performance at high γ_S (i.e. $\gamma_S \rightarrow \infty$). With finite μ , we nearly have $\mu_m = \min\{\mu, \gamma_S L_{SR}^{-\alpha} N\} = \mu$. Herein, we do not consider the case of high γ_R because the instantaneous increase in N and γ_R is obviously costly and impractical. Once N is large, γ_R had better be low to reduce the power consumption per antenna at R.

1) *AF scheme:* We consider the following terms:

$$\begin{aligned} \mathbb{T}(l) &\triangleq \lim_{\gamma_S \rightarrow \infty} \mathcal{T}_{\mu_m}(l) \mathbb{1}(\mu_m < \gamma_S L_{SR}^{-\alpha} N) \\ &= \lim_{\gamma_S \rightarrow \infty} \exp \left\{ \frac{(1 + \gamma_S L_{SR}^{-\alpha} N) \mu}{\gamma_R l^{-\alpha} (\mu - \gamma_S L_{SR}^{-\alpha} N)} \right\} \\ &= \exp \left\{ -\mu / (\gamma_R l^{-\alpha}) \right\} \end{aligned} \quad (51)$$

and

$$\begin{aligned} \mathbb{J}(l) &\triangleq \lim_{\gamma_S \rightarrow \infty} \frac{\gamma_S L_{SR}^{-\alpha} N (1 + \gamma_S L_{SR}^{-\alpha} N)}{\gamma_R l^{-\alpha}} \mathcal{J}_{\mu_m}(l, l_{SE}) \\ &= \frac{(\gamma_S L_{SR}^{-\alpha} N)^2}{\gamma_R l^{-\alpha}} \int_0^{\mu} \frac{e^{\frac{\gamma_S L_{SR}^{-\alpha} N x}{\gamma_R l^{-\alpha} (-\gamma_S L_{SR}^{-\alpha} N)}}}{(\gamma_S L_{SR}^{-\alpha} N)^2} dx \\ &= 1 - \exp \left\{ -\mu / (\gamma_R l^{-\alpha}) \right\}. \end{aligned} \quad (52)$$

$$\begin{aligned} \text{SOP}_\mu^{AF} = 1 - \exp \left\{ -\lambda \int_0^{2\pi} \int_0^{R_\Psi} \left[\exp \left\{ \frac{(1 + \gamma_S L_{SR}^{-\alpha} N) \mu_m}{\gamma_R l^{-\alpha} (\mu_m - \gamma_S L_{SR}^{-\alpha} N)} \right\} \mathbb{1}(\mu_m < \gamma_S L_{SR}^{-\alpha} N) \right. \right. \\ \left. \left. + \frac{\gamma_S L_{SR}^{-\alpha} N (1 + \gamma_S L_{SR}^{-\alpha} N)}{\gamma_R l^{-\alpha}} \exp \left\{ \frac{-\mu}{\gamma_S (L_{SR}^2 + l^2 - 2L_{SR} l \cos \phi)^{-\alpha/2}} \right\} \right. \right. \\ \left. \left. \times \int_0^{\mu_m} \frac{\exp \left\{ \frac{x}{\gamma_S (L_{SR}^2 + l^2 - 2L_{SR} l \cos \phi)^{-\alpha/2}} + \frac{(1 + \gamma_S L_{SR}^{-\alpha} N) x}{\gamma_R l^{-\alpha} (x - \gamma_S L_{SR}^{-\alpha} N)} \right\}}{(x - \gamma_S L_{SR}^{-\alpha} N)^2} dx \right] l dl d\phi \right\} \quad (49) \end{aligned}$$

$$\begin{aligned} \text{SOP}_\mu^{DF} = 1 - \exp \left\{ -\lambda \int_0^{2\pi} \int_0^{R_\Psi} \left[e^{-\frac{\mu_m}{\gamma_R l^{-\alpha}}} - e^{-\frac{\gamma_S L_{SR}^{-\alpha} N}{\gamma_R l^{-\alpha}}} \left(1 - e^{-\frac{\mu_m - \mu}{\gamma_S (L_{SR}^2 + l^2 - 2L_{SR} l \cos \phi)^{-\alpha/2}}} \right) \mathbb{1}(\mu > \gamma_S L_{SR}^{-\alpha} N) \right. \right. \\ \left. \left. - \frac{\gamma_S (L_{SR}^2 + l^2 - 2L_{SR} l \cos \phi)^{-\alpha/2}}{\gamma_R l^{-\alpha} - \gamma_S (L_{SR}^2 + l^2 - 2L_{SR} l \cos \phi)^{-\alpha/2}} \exp \left\{ -\frac{\mu}{\gamma_S (L_{SR}^2 + l^2 - 2L_{SR} l \cos \phi)^{-\alpha/2}} \right\} \right. \right. \\ \left. \left. \times \left(1 - \exp \left\{ \mu_m \left(\frac{1}{\gamma_S (L_{SR}^2 + l^2 - 2L_{SR} l \cos \phi)^{-\alpha/2}} - \frac{1}{\gamma_R l^{-\alpha}} \right) \right\} \right) \right] l dl d\phi \right\} \quad (55) \end{aligned}$$

Taking limit (40) at $\gamma_S \rightarrow \infty$, we have

$$\lim_{\gamma_S \rightarrow \infty} F_{\text{snr}_E^{AF}}(\mu) = 1 - \mathbb{T}(l) - \mathbb{J}(l) = 0. \quad (53)$$

Then using the two above-calculated limits, we reach the limit of $\mathbb{P} \{ \Lambda_E^{AF} \}$ in (48) at $\gamma_S \rightarrow \infty$ as follows:

$$\begin{aligned} \text{SOP}_{\mu, \text{asym}}^{AF} &= \lim_{\gamma_S \rightarrow \infty} \text{SOP}_\mu^{AF} \\ &= 1 - \exp \left\{ -\lambda \int_0^{2\pi} \int_0^{R_\Psi} (1 - 0) l dl d\phi \right\} \\ &= 1 - \exp \{ -\pi \lambda R_\Psi^2 \}. \quad (54) \end{aligned}$$

2) *DF scheme*: Taking limit (44) at $\gamma_S \rightarrow \infty$, we have

$$\begin{aligned} \lim_{\gamma_S \rightarrow \infty} F_{\text{snr}_E^{DF}}(\mu) &= 1 - e^{-\frac{\mu_m}{\gamma_R l^{-\alpha}}} + \frac{\gamma_S l_{SE}^{-\alpha}}{(-\gamma_S l_{SE}^{-\alpha})} \left(1 - e^{-\frac{\mu_m}{\gamma_R l^{-\alpha}}} \right) \\ &= 0. \quad (56) \end{aligned}$$

Then, the limitation of (50) is given by

$$\begin{aligned} \text{SOP}_{\mu, \text{asym}}^{DF} &= \lim_{\gamma_S \rightarrow \infty} \text{SOP}_\mu^{DF} \\ &= 1 - \exp \left\{ -\lambda \int_0^{2\pi} \int_0^{R_\Psi} (1 - 0) l dl d\phi \right\} \\ &= 1 - \exp \{ -\pi \lambda R_\Psi^2 \}. \quad (57) \end{aligned}$$

Remark 1. We observe from (54) and (57) that when γ_S increases, the role of the considered relaying operations comes to be indistinguishable since both AF and DF cases give the same value at high γ_S . Indeed, this observation can also be realized in a more intuitive manner: First, we take the limit of (35), i.e.,

$$\begin{aligned} \lim_{\gamma_S \rightarrow \infty} \text{snr}_E^{AF} &= \lim_{\gamma_S \rightarrow \infty} \left\{ \frac{\gamma_S L_{SR}^{-\alpha} \gamma_R l^{-\alpha} N \Theta}{\gamma_S L_{SR}^{-\alpha} N} \right\} + \gamma_S l_{SE}^{-\alpha} |h_{SE}|^2 \\ &= \gamma_R l^{-\alpha} \Theta + \gamma_S l_{SE}^{-\alpha} |h_{SE}|^2, \\ \lim_{\gamma_S \rightarrow \infty} \text{snr}_E^{DF} &= \lim_{\gamma_S \rightarrow \infty} \left\{ \min \{ \gamma_S L_{SR}^{-\alpha} N, \gamma_R l^{-\alpha} \Theta \} + \gamma_S l_{SE}^{-\alpha} |h_{SE}|^2 \right\} \\ &= \gamma_R l^{-\alpha} \Theta + \gamma_S l_{SE}^{-\alpha} |h_{SE}|^2. \quad (58) \end{aligned}$$

Then taking the limit of SOP_μ^{AF} in (49) and SOP_μ^{DF} in (55), we arrive at the same conclusion, i.e. $\lim_{\gamma_S \rightarrow \infty} \text{SOP}_\mu^{AF} = \lim_{\gamma_S \rightarrow \infty} \text{SOP}_\mu^{DF}$.

Proposition 3. For given μ , both SOP_μ^{AF} and SOP_μ^{DF} increase with γ_S . Furthermore, they are upper bounded by the limit $1 - \exp \{ -\pi \lambda R_\Psi^2 \}$, which increases with λ as well as R_Ψ . In this respect, we can conclude that when the eavesdroppers' density λ becomes denser or their working range R_Ψ becomes wider, the upper limit of the SOP in two relaying cases will be higher accordingly.

Proof. Please see Appendix C. \square

V. CONNECTION OUTAGE PROBABILITY (COP)

To deal with the attacks from eavesdroppers as well as restrict information leakage to a certain extent, we consider an on-off transmission strategy (a recent paper [32] as an example). As for this strategy, some threshold η is compared to the instantaneous SNR at D before the transmission is performed. More precisely, if $\widehat{\text{SNR}}_D \leq \eta$, then S had better keep silent (OFF-state); in contrast, S will transmit confidential signals (ON-state). As such, the transmission will be in the OFF-state with the probability $\mathbb{P} \{ \widehat{\text{SNR}}_D \leq \eta \}$ which can be named as the COP, i.e.

$$\widehat{\text{COP}}_\eta \equiv \mathbb{P} \{ \text{OFF-state} \} \triangleq \mathbb{P} \{ \widehat{\text{SNR}}_D \leq \eta \}. \quad (59)$$

A. Analysis with large N

Under the assumption of (very) large N , we can use (59), (34) and (36) to arrive at the following approximation

$$\widehat{\text{COP}}_\eta \xrightarrow{N \rightarrow \infty} \text{COP}_\eta = \mathbb{P} \{ \text{snr}_D \leq \eta \}. \quad (60)$$

In the following, we analyze the COP for the AF scheme and the DF scheme, respectively.

1) *AF scheme*: We replace snr_D with snr_D^{AF} into the above expression to obtain the COP for the AF case, i.e.

$$\begin{aligned} \text{COP}_\eta^{AF} &= \mathbb{P} \left\{ \text{snr}_D^{AF} \leq \eta \right\} \\ &= \mathbb{P} \left\{ \frac{\gamma_S L_{SR}^{-\alpha} \gamma_R L_{RD}^{-\alpha} N^2}{\gamma_S L_{SR}^{-\alpha} N + \gamma_R L_{RD}^{-\alpha} N + 1} \leq \eta \right\} \\ &= \mathbb{P} \left\{ \gamma_S L_{SR}^{-\alpha} N (\gamma_R L_{RD}^{-\alpha} N - \eta) \leq \eta (\gamma_R L_{RD}^{-\alpha} N + 1) \right\} \\ &= \begin{cases} 1, & \text{if } \gamma_R \leq \Omega_\eta \\ \mathbb{P} \left\{ \gamma_S \leq \frac{\eta (\gamma_R L_{RD}^{-\alpha} N + 1)}{L_{SR}^{-\alpha} N (\gamma_R L_{RD}^{-\alpha} N - \eta)} \right\}, & \text{if } \gamma_R > \Omega_\eta \end{cases} \\ &= \begin{cases} 1, & \text{if } \gamma_R \leq \Omega_\eta \\ 1, & \text{if } \gamma_R > \Omega_\eta \text{ and } \gamma_S \leq \Upsilon_\eta \\ 0, & \text{if } \gamma_R > \Omega_\eta \text{ and } \gamma_S > \Upsilon_\eta \end{cases} \end{aligned} \quad (61)$$

where

$$\Omega_\eta \triangleq \eta / (N L_{RD}^{-\alpha}), \quad (62)$$

$$\Upsilon_\eta \triangleq \frac{\eta (\gamma_R L_{RD}^{-\alpha} N + 1)}{L_{SR}^{-\alpha} L_{RD}^{-\alpha} N^2 (\gamma_R - \Omega_\eta)}. \quad (63)$$

There is no surprise that the COP takes only two values, either 1 or 0, due to the fact that all parameters γ_S , γ_R , N , α , L_{SR} , L_{RD} , and η are predetermined. From the design perspective, we want $\text{COP}_\eta = 0$ because it implies that the confidential transmission can occur (in the ON-state). As such, considering the on-off transmission strategy, designers must make sure that the two following conditions hold true:

$$\begin{cases} \gamma_R > \Omega_\eta \\ \gamma_S > \Upsilon_\eta \end{cases}. \quad (64)$$

2) *DF scheme*: With snr_D^{DF} substituted for snr_D in (60), the COP for the DF case can be calculated as

$$\begin{aligned} \text{COP}_\eta^{DF} &= \mathbb{P} \left\{ \text{snr}_D^{DF} \leq \eta \right\} \\ &= \mathbb{P} \left\{ \min \left\{ \gamma_S L_{SR}^{-\alpha} N, \gamma_R L_{RD}^{-\alpha} N \right\} \leq \eta \right\} \\ &= \begin{cases} 1, & \text{if } \gamma_S \leq \omega_\eta \text{ and } \gamma_S \leq \gamma_R (L_{RD}/L_{SR})^{-\alpha} \\ 0, & \text{if } \gamma_S > \omega_\eta \text{ and } \gamma_S \leq \gamma_R (L_{RD}/L_{SR})^{-\alpha} \\ 1, & \text{if } \gamma_R \leq \Omega_\eta \text{ and } \gamma_S > \gamma_R (L_{RD}/L_{SR})^{-\alpha} \\ 0, & \text{if } \gamma_R > \Omega_\eta \text{ and } \gamma_S > \gamma_R (L_{RD}/L_{SR})^{-\alpha} \end{cases} \end{aligned} \quad (65)$$

where

$$\omega_\eta \triangleq \eta / (N L_{SR}^{-\alpha}). \quad (66)$$

Similarly to the AF case, we wish to have $\text{COP}_\eta = 0$, then

$$\begin{cases} \text{either } \Omega_\eta < \gamma_R < \gamma_S (L_{SR}/L_{RD})^{-\alpha} \\ \text{or } \omega_\eta < \gamma_S \leq \gamma_R (L_{RD}/L_{SR})^{-\alpha}, \end{cases} \quad (67)$$

needs to be satisfied.

B. Analysis with large N and high γ_S

As analyzed in the last subsection, we need to set the values of γ_S , γ_R and N such that the COP is equal to 0 for each relaying strategy at R. With high γ_S (i.e. $\gamma_S \rightarrow \infty$) the second condition in (64) is almost surely true, because $\lim_{\gamma_S \rightarrow \infty} \mathbb{P} \left\{ \gamma_S > \Upsilon_\eta \right\} = 1$; thus, the COP in the AF case will approach 0 (i.e. the OFF-state does not occur) at high γ_S given that the first condition in (64) is satisfied. Meanwhile, the

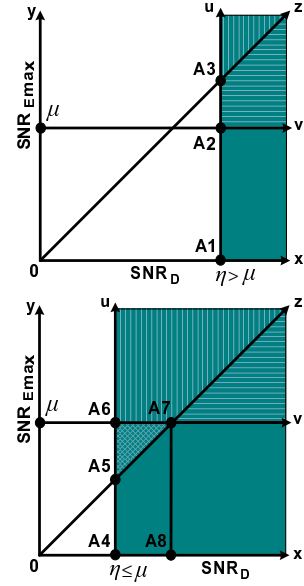


Fig. 2. Possible insecure/secured states of the proposed system versus corresponding ranges of $(\text{snr}_D, \text{snr}_{E\max})$.

second condition in (67) does not seem to be achievable at high γ_S ; thus, the COP can reach 0 as long as the first condition in (67) is satisfied. In short, the OFF-state occurs at high γ_S when $\Omega_\eta < \gamma_R$ for AF scheme and $\Omega_\eta < \gamma_R < \gamma_S (L_{SR}/L_{RD})^{-\alpha}$ for DF scheme.

VI. SECURITY-RELIABILITY TRADEOFF

In this section, we evaluate the interactions of the important secure metrics including the SOP, the COP and the end-to-end (e2e) SR. It is of importance that the SOP and the COP will be jointly evaluated in another probabilistic metric, i.e. the probability of achieving the most secured transmission state $\mathbb{P}\{\hat{\mathcal{A}}\}$. With (very) large N , we have $\mathbb{P}\{\hat{\mathcal{A}}\} \xrightarrow{N \rightarrow \infty} \mathbb{P}\{\mathcal{A}\}$; while the e2e SR (in nats/s/Hz) can be expressed as $C_s = \frac{1}{2} \max \left\{ \ln \left(\frac{1 + \text{snr}_D}{1 + \text{snr}_{E\max}} \right), 0 \right\}$ where 1/2 is due to the fact that the transmission is divided into two equal time slots. All metrics C_s , SOP_μ and COP_η involve the same parameter γ_S ; thus, we respectively rewrite C_s , SOP_μ and COP_η as $C_s(\gamma_S)$, $\text{SOP}_\mu(\gamma_S)$ and $\text{COP}_\eta(\gamma_S)$ to emphasize the role of γ_S in our analysis for the rest of this paper.

Now, let us look at Fig. 2 which is provided for illustration. In the figure, there are two regions for the e2e SR, the region $y0z$ corresponds to $C_s(\gamma_S) = 0$ (i.e. $\text{snr}_D \leq \text{snr}_{E\max}$), the region $x0z$ corresponds to $C_s(\gamma_S) > 0$ (i.e. $\text{snr}_D > \text{snr}_{E\max}$). Still in Fig. 2, we consider the two scenarios of η as follows:

- With $\eta > \mu$, the transmission only occurs in the ON-state ($\text{COP}_\eta(\gamma_S) = 0$) if a pair of $(\text{snr}_D, \text{snr}_{E\max})$ lies in the region uA_1x . In this case, there are 3 subcases corresponding to 3 regions:
 - uA_3z has $C_s(\gamma_S) = 0$ and $\text{snr}_{E\max} \geq \mu$.
 - zA_3A_2v has $C_s(\gamma_S) > 0$ and $\text{snr}_{E\max} \geq \mu$.
 - vA_2A_1x has $C_s(\gamma_S) > 0$ and $\text{snr}_{E\max} < \mu$.

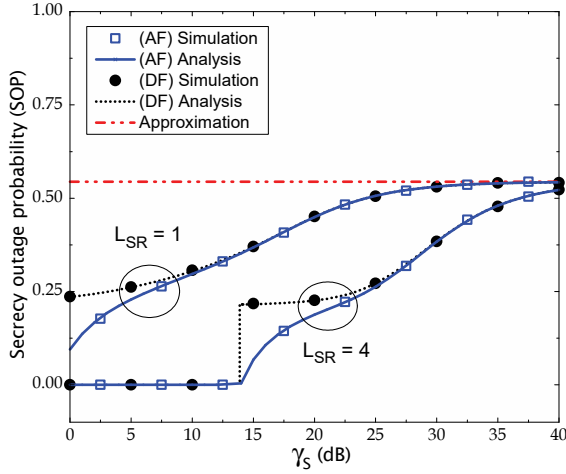


Fig. 3. SOP_{μ}^{AF} in (49) and SOP_{μ}^{DF} in (55) versus γ_S . For each relaying scheme, two subcases are considered: $L_{SR} = 1$ and $L_{SR} = 4$. Other parameters: $N = 50$, $\lambda = 0.25$, $R_{\Psi} = 1$, $\alpha = 2.5$, $\gamma_R = 10$ dB, $\mu = 16.02$ dB.

- With $\eta \leq \mu$, the transmission only occurs (in the ON-state) if the considered pair of instantaneous SNRs lies in the region uA_4x . In this case, there are 4 subcases:
 - uA_6A_7z has $C_s(\gamma_S) = 0$ and $\text{snr}_{Emax} \geq \mu$.
 - zA_7v has $C_s(\gamma_S) > 0$ and $\text{snr}_{Emax} \geq \mu$.
 - $A_5A_6A_7$ has $C_s(\gamma_S) = 0$ and $\text{snr}_{Emax} < \mu$.
 - $vA_7A_5A_4x$ has $C_s(\gamma_S) > 0$ and $\text{snr}_{Emax} < \mu$.

Obviously, if we have $(\text{snr}_D, \text{snr}_{Emax}) \in vA_2A_1x$ in the case of $\eta > \mu$ and/or $(\text{snr}_D, \text{snr}_{Emax}) \in vA_7A_5A_4x$ in the case of $\eta \leq \mu$, the proposed system will attain the most secured state with $C_s(\gamma_S) > 0$, $COP_{\mu}(\gamma_S) = 0$ and $\text{snr}_{Emax} < \mu$. We only focus on the case of $\eta > \mu$ in this paper and evaluate the probability of the event $\mathcal{A} = \{(\text{snr}_D, \text{snr}_{Emax}) \in vA_2A_1x\}$. Of course, this event is the expected one because the security state of our system is guaranteed at most. The probability of the occurrence of the event \mathcal{A} is given by

$$\begin{aligned} \mathbb{P}\{\mathcal{A}\} &= \mathbb{P}\{(\text{snr}_D, \text{snr}_{Emax}) \in vA_2A_1x \mid \eta > \mu\} \\ &= \mathbb{P}\{\eta < \text{snr}_D, \text{snr}_{Emax} < \mu\} \\ &= \mathbb{P}\left\{\max_{Ei \in \Psi} \text{snr}_E < \mu\right\} \mathbb{P}\{\eta < \text{snr}_D\} \\ &= [1 - SOP_{\mu}(\gamma_S)] [1 - COP_{\eta}(\gamma_S)]. \end{aligned} \quad (68)$$

We will denote $\mathbb{P}\{\mathcal{A}\}$ as $\mathbb{P}\{\mathcal{A}\}^{AF}$ and $\mathbb{P}\{\mathcal{A}\}^{DF}$ for the AF case and DF case, respectively.

A. AF case

In order to maximize the probability $\mathbb{P}\{\mathcal{A}\}^{AF}$, we aim to solve the following optimization problem:

$$\begin{aligned} (\mathbf{P}^{AF}) \quad & \underset{\gamma_S}{\text{minimize}} \quad SOP_{\mu}^{AF}(\gamma_S) \\ & \text{subject to} \quad COP_{\eta}^{AF}(\gamma_S) = 0. \end{aligned}$$

Using (64), the constraint turns out to be $\gamma_R > \Omega_{\eta}$ and $\gamma_S > \Upsilon_{\eta}$. Once the constraint $\gamma_R > \Omega_{\eta}$ is satisfied, (\mathbf{P}^{AF}) has the optimal solution

$$\gamma_{S,opt} \rightarrow \Upsilon_{\eta}^+ \quad (69)$$

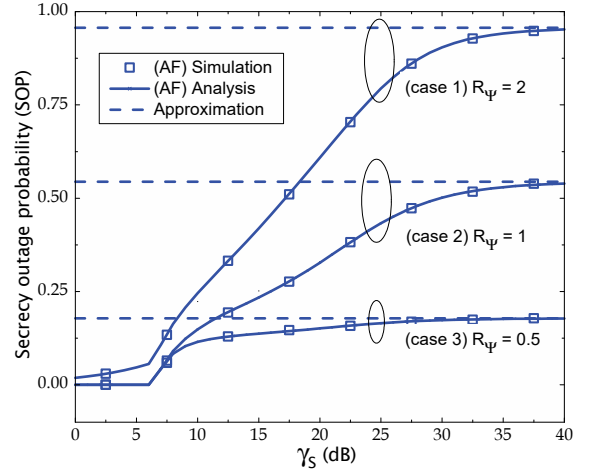


Fig. 4. SOP_{μ}^{AF} in (49) versus γ_S . For each relaying scheme, two subcases are considered: (case 1) $R_{\Psi} = 2$; (case 2) $R_{\Psi} = 1$; and (case 3) $R_{\Psi} = 0.5$. Other parameters: $N = 50$, $\lambda = 0.25$, $L_{SR} = 2$, $\alpha = 2.5$, $\gamma_R = 10$ dB, $\mu = 16.02$ dB.

because $SOP_{\mu}^{AF}(\gamma_S) > SOP_{\mu}^{AF}(\Upsilon_{\eta})$ for all $\gamma_S > \Upsilon_{\eta}$ (according to Proposition 3). In contrast, if the constraint $\gamma_R > \Omega_{\eta}$ is not satisfied, the event \mathcal{A} does not occur regardless of any value of γ_S . As such, we have

$$\max_{\gamma_S} \mathbb{P}\{\mathcal{A}\}^{AF} = \begin{cases} 1 - SOP_{\mu}^{AF}(\Upsilon_{\eta}^+), & \text{if } \gamma_R > \Omega_{\eta} \\ 0, & \text{if } \gamma_R \leq \Omega_{\eta} \end{cases}. \quad (70)$$

B. DF case

In the same way as the AF case, we suggest the optimization problem for the DF case as follows:

$$\begin{aligned} (\mathbf{P}^{DF}) \quad & \underset{\gamma_S}{\text{minimize}} \quad SOP_{\mu}^{DF}(\gamma_S) \\ & \text{subject to} \quad COP_{\eta}^{DF}(\gamma_S) = 0. \end{aligned}$$

Using (67), the constraint becomes $\Omega_{\eta} < \gamma_R < \gamma_S (L_{SR}/L_{RD})^{-\alpha}$ or $\omega_{\eta} < \gamma_S \leq \gamma_R (L_{RD}/L_{SR})^{-\alpha}$. Moreover, $SOP_{\mu}(\gamma_S)$ increases with γ_S , then the problem (\mathbf{P}^{DF}) has two optimal solutions:

$$\gamma_{S,opt} = \begin{cases} \gamma_R^+ (L_{RD}/L_{SR})^{-\alpha}, & \text{if } \gamma_R > \Omega_{\eta} \\ \omega_{\eta}^+, & \text{if } \gamma_R \geq \omega_{\eta}^+ (L_{SR}/L_{RD})^{-\alpha} \triangleq \varpi \end{cases}. \quad (71)$$

Finally, the maximal value of $\mathbb{P}\{\mathcal{A}\}^{DF}$ can be readily deduced from (71) as follows:

$$\begin{aligned} \max_{\gamma_S} \mathbb{P}\{\mathcal{A}\}^{DF} &= \begin{cases} \max\left\{\mathbb{P}\{\mathcal{A}\}_{opt,1}^{DF}, \mathbb{P}\{\mathcal{A}\}_{opt,1}^{DF}\right\}, & \text{if } \Omega_{\eta} < \varpi \leq \gamma_R \\ & \text{or } \gamma_R > \Omega_{\eta} \geq \varpi, \\ \mathbb{P}\{\mathcal{A}\}_{opt,1}^{DF}, & \text{if } \Omega_{\eta} < \gamma_R < \varpi, \\ \mathbb{P}\{\mathcal{A}\}_{opt,2}^{DF}, & \text{if } \Omega_{\eta} \geq \gamma_R \geq \varpi, \\ 0, & \text{if } \gamma_R \leq \Omega_{\eta} < \varpi \\ & \text{or } \Omega_{\eta} \geq \varpi > \gamma_R \end{cases} \end{aligned} \quad (72)$$

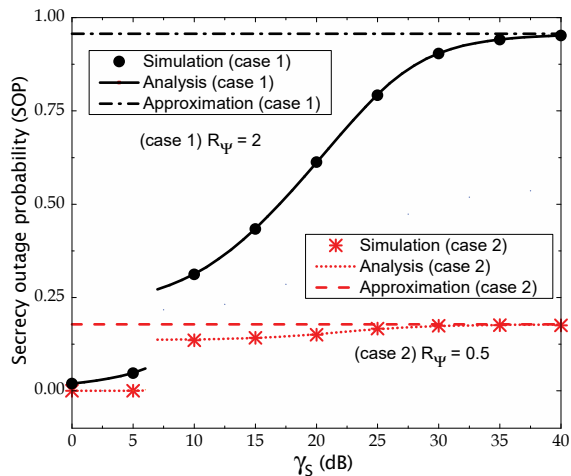


Fig. 5. SOP_{μ}^{DF} in (55) versus γ_S . For each relaying scheme, two subcases are considered: (case 1) $R_{\Psi} = 2$; (case 2) $R_{\Psi} = 0.5$. Other parameters: $N = 50$, $\lambda = 0.25$, $L_{SR} = 2$, $\alpha = 2.5$, $\gamma_R = 10$ dB, $\mu = 16.02$ dB.

where $\mathbb{P}\{\mathcal{A}\}_{opt,1}^{DF} \triangleq 1 - SOP_{\mu}^{DF}(\gamma_S) \Big|_{\gamma_S=\omega_{\eta}^+}$ and $\mathbb{P}\{\mathcal{A}\}_{opt,2}^{DF} \triangleq 1 - SOP_{\mu}^{DF}(\gamma_S) \Big|_{\gamma_S=\gamma_R^+(L_{RD}/L_{SR})^{-\alpha}}$.

Remark 2. Both cases require the cooperation between S and R such that γ_S and γ_R meet the requirement for quality of service (i.e. $\mathbb{P}\{\mathcal{A}\}$ is maximized). When the parameter γ_R is beforehand chosen, we only need to set up the parameter γ_S to reach the goal. Hence, we choose $\gamma_R > \Omega_{\eta}$ in the AF case; meanwhile, γ_R should satisfy either $\Omega_{\eta} < \varpi \leq \gamma_R$ or $\gamma_R > \Omega_{\eta} \geq \varpi$ in the DF case.

VII. NUMERICAL RESULTS

This section provides several numerical examples to verify the correctness of our analysis and show secure characteristics of the proposed system. Relating to distance parameters, the distance reference R_0 is traditionally selected from 100 m to 1 km for large cellular systems [22]–[24]. With the selection of R_0 within $[100m, 1000m]$, the measurement unit of λ will be implicitly understood as the average number of eavesdroppers over $R_0 \times R_0$ m². Note that the selected value of R_0 does not change our numerical results, which depend on the distance ratios L_{SR} , L_{RD} and R_{Ψ} . Furthermore, a suitable value of the path loss exponent α should be from 2 to 3. Thus, we choose to set $\alpha = 2.5$ for all numerical examples. Finally, it is of crucial importance that all simulation results have been performed for \widehat{SOP}_{μ} , \widehat{COP}_{η} and $\mathbb{P}\{\mathcal{A}\}$; whereas, all analytical results have been performed for SOP_{μ} , COP_{η} and $\mathbb{P}\{\mathcal{A}\}$.

In Figs. 3–5, we present the SOPs versus γ_S in the AF and DF scheme. The analytical expressions for the SOP are verified through simulation, i.e. $\widehat{SOP}_{\mu} \xrightarrow{N \rightarrow \infty} SOP_{\mu}$ and $\widehat{SOP}_{\mu} \xrightarrow{N, \gamma_S \rightarrow \infty} SOP_{\mu, asym}$ are confirmed. As seen from the figures, the simulated values of \widehat{SOP}_{μ} and the analytical values of SOP_{μ} match each other at large N (i.e. $N = 50$) through the range $[0, 40]$ dB of γ_S . Besides, these values increase with γ_S and converges to $SOP_{\mu, asym}$ at high γ_S (for example, at 40 dB).

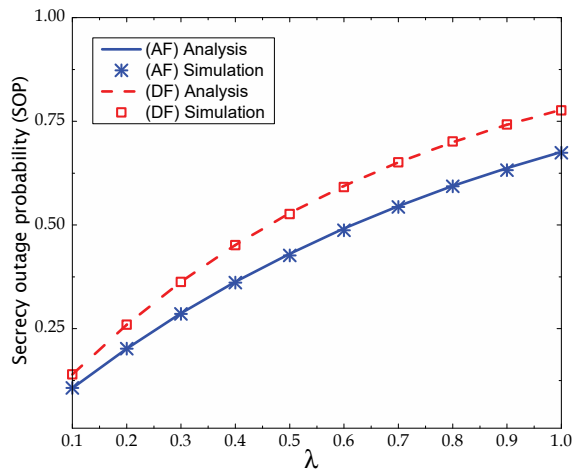


Fig. 6. SOP_{μ}^{AF} in (49) and SOP_{μ}^{DF} in (55) versus λ . Parameters: $N = 50$, $R_{\Psi} = 2$, $L_{SR} = 2$, $\alpha = 2.5$, $\gamma_S = 10$ dB, $\gamma_R = 10$ dB, $\mu = 16.02$ dB.

In Fig. 3, two subcases of L_{SR} are considered, i.e. $L_{SR} = \{1, 4\}$. We can see that the security performance in AF case is better than DF case for each considered value of L_{SR} . However, when γ_S exceeds over 15 dB for the case of $L_{SR} = 1$, the security performance in the AF scheme and that in the DF scheme is the same and thereby, the role of the relaying protocols becomes indistinguishable. Interestingly, the decrease in L_{SR} (i.e. S comes closer to R) does not ensure that the secure performance will be improved.

Regarding Figs. 4–5, we fix the distance ratio L_{SR} and change the radius ratio R_{Ψ} . We observe that the secure performance inversely decreases with the increase in R_{Ψ} . This observation can also be recorded from the practice that with the working range extension, the eavesdroppers will become more dangerous. In Fig. 6, we depict the SOPs versus λ . Again, the results confirm again that the AF scheme gives better secure performance. Moreover, the difference in performance between two schemes becomes less with the increase in γ_S . Besides, the increasing density of eavesdroppers also causes a worse situation for the proposed system (as can be observed intuitively).

In Fig. 7, we depict the COPs versus γ_S in the AF case and verify $\widehat{COP}_{\mu}^{AF} \xrightarrow{N \rightarrow \infty} COP_{\mu}^{AF}$. The results show that when N increases, our analysis becomes more precise because the gap between simulation curve (i.e. $\widehat{COP}_{\eta}^{AF}$) and analytical curve (i.e. COP_{η}^{AF}) is narrowed. In the case of $N = 40$, the first constraint $\gamma_R > \Omega_{\eta}$ is satisfied, i.e. $\gamma_R = 10$ dB $>$ 8.38 dB, then the COP theoretically reaches 0 at any $\gamma_R > \Upsilon_{\eta} \approx 16.6$ dB. Likewise, in the case of $N = 70$, the constraint $\gamma_R \approx 13.01$ dB $>$ 5.95 dB, then the COP is expected to be 0 at any $\gamma_R > \Upsilon_{\eta} \approx 11.26$ dB. In comparison between two cases, we can see that the increase in N helps to enhance the reliability. For example, if the secure transmission occurs at $\gamma_S = 15$ dB, then $N = 70$ will be selected because the theoretical COP equals 0; in contrast, $N = 40$ will lead to an unsecured transmission as the theoretical SOP is 1.

In Fig. 8, we depict the COPs versus γ_S in the DF case. Similar to the AF case, the gap between the analysis and

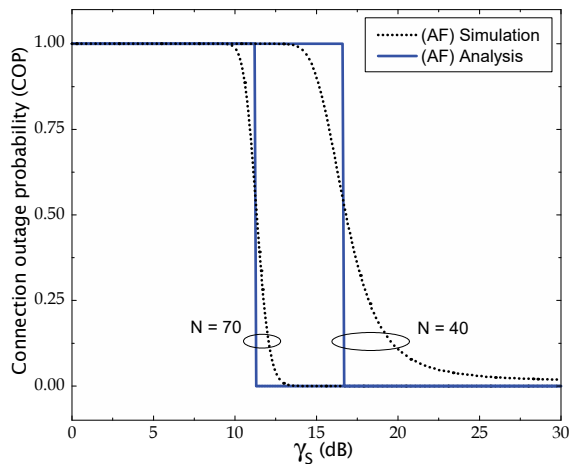


Fig. 7. COP_η^{AF} versus γ_S . Parameters: $N = \{40, 70\}$, $L_{SR} = 2$, $L_{RD} = 1.5$, $\alpha = 2.5$, $\gamma_R = 10$ dB, $\eta = 20$ dB.

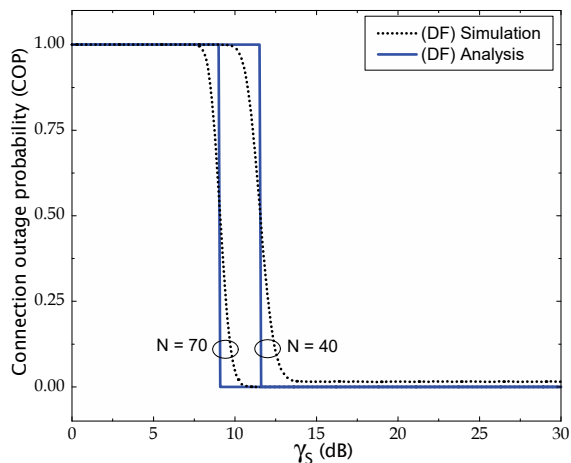


Fig. 8. COP_η^{DF} versus γ_S . Parameters: $N = \{40, 70\}$, $L_{SR} = 2$, $L_{RD} = 1.5$, $\alpha = 2.5$, $\gamma_R = 10$ dB, $\eta = 20$ dB.

simulation becomes more precise when N increases. Moreover, if one of the two conditions in (67) is satisfied, the COP reaches 0. For example, in the case of $N = 40$, the condition $\Omega_\eta \approx 10^{8.38/10} < \gamma_R = 10^{10/10}$ dB $< \gamma_S (2/1.5)^{-2.5}$ can be attained if $\gamma_S > 13.12$ dB. In the case $N = 70$, the condition $\omega_\eta \approx 10^{9.07/10} < \gamma_S \leq 10^{10/10} (1.5/2)^{-2.5} \Leftrightarrow 9.07$ dB $< \gamma_S \leq 13.12$ dB will lead to $\text{COP}_\eta^{DF} = 0$.

In Fig. 9, the probability of the most secured state $\mathbb{P}\{\mathcal{A}\}^{AF}$ is shown with respect to γ_S . The results show that the agreement between the analytical curves and the simulation curves can be obtained with N increased. We can see that with $N = 50$, we have $\mathbb{P}\{\mathcal{A}\}^{AF} > 0$ at any $\gamma_S > 21$ dB. In contrast, to have $\mathbb{P}\{\mathcal{A}\}^{AF} > 0$ in the case of $N = 70$, we have to set $\gamma_S > 19$ dB. As such, the increase in N helps ensure $\mathbb{P}\{\mathcal{A}\}^{AF} > 0$ when γ_S decreases. As analyzed in Section VI, $\mathbb{P}\{\mathcal{A}\}^{AF}$ reaches its maximum when $\gamma_S \rightarrow \Upsilon_\eta^+$. For example, in theoretical perspective, with $N = 70$ we have $\max_{\gamma_S} \mathbb{P}\{\mathcal{A}\}^{AF} = \mathbb{P}\{\mathcal{A}\}^{AF} |_{\gamma_S = \Upsilon_\eta + \epsilon} \approx 0.811$ where ϵ is a very small positive number. Likewise, in Fig. 10, the probability of the most secured state $\mathbb{P}\{\mathcal{A}\}^{DF}$ is also

illustrated with γ_S . The behaviour of $\mathbb{P}\{\mathcal{A}\}^{DF}$ is similar to $\mathbb{P}\{\mathcal{A}\}^{AF}$. The increase in N makes the secure performance more guaranteed as long as the transmission state is in the ON-state.

VIII. CONCLUSIONS

In this paper, we have considered a relay-aided wireless system with the large antenna array equipped at the relay. In the presence of many potential eavesdroppers, we assume that they follow a homogeneous PPP. Furthermore, compared to the destination, all eavesdroppers have much more advantages when direct links between them and the source are discussed. Under such assumptions, we have employed the ON-OFF strategy and evaluated the security as well as the reliability of the system through probabilistic metrics. Analysis and simulation results show that the increase in γ_S reduces the secure performance in both AF and DF case. The increase in γ_S , however, helps enhance the reliability in both the AF case and the DF case. Finally, two appropriate optimization problems have been proposed for each relaying scheme such that the probability of achieving the most secured state in each transmission is optimal. On the other side, a large value of N makes the COP reach 0, which means that a secured transmission can occur thanks to the increase in N .

APPENDIX

A. The CDF of snr_E^{AF}

Let us define $\mathcal{X} = \frac{\gamma_S L_{SR}^{-\alpha} \gamma_R l^{-\alpha} N \Theta}{(\gamma_S L_{SR}^{-\alpha} N + 1) + \gamma_R l^{-\alpha}}$. The CDF and PDF of \mathcal{X} can be, respectively, calculated as

$$\begin{aligned} F_{\mathcal{X}}(x) &= \mathbb{P}\left\{(\gamma_S L_{SR}^{-\alpha} N - x)\gamma_R l^{-\alpha} \Theta \leq (\gamma_S L_{SR}^{-\alpha} N + 1)x\right\} \\ &= 1 - \exp\left\{-\frac{(1 + \gamma_S L_{SR}^{-\alpha} N)x}{\gamma_R l^{-\alpha}(x - \gamma_S L_{SR}^{-\alpha} N)}\right\} \mathbb{1}(x < \gamma_S L_{SR}^{-\alpha} N) \end{aligned} \quad (73)$$

and

$$\begin{aligned} f_{\mathcal{X}}(x) &= \exp\left\{-\frac{(1 + \gamma_S L_{SR}^{-\alpha} N)x}{\gamma_R l^{-\alpha}(x - \gamma_S L_{SR}^{-\alpha} N)}\right\} \\ &\quad \times \frac{\gamma_S L_{SR}^{-\alpha} N(1 + \gamma_S L_{SR}^{-\alpha} N)}{\gamma_R l^{-\alpha}(x - \gamma_S L_{SR}^{-\alpha} N)^2} \mathbb{1}(x < \gamma_S L_{SR}^{-\alpha} N). \end{aligned} \quad (74)$$

As such, snr_E^{AF} in (35) is rewritten as $\text{snr}_E^{AF} = \gamma_S l_{SE}^{-\alpha} |h_{SE}|^2 + \mathcal{X}$. The CDF of snr_E^{AF} is given by

$$F_{\text{snr}_E^{AF}}(\mu) = \int_0^{\mu_m} F_{|h_{SE}|^2} \left(\frac{\mu - x}{\gamma_S l_{SE}^{-\alpha}} \right) f_{\mathcal{X}}(x) dx \quad (75)$$

where $\mu_m \triangleq \min\{\mu, \gamma_S L_{SR}^{-\alpha} N\}$. After some manipulations, (75) is expressed in the form of (40).

B. The CDF of snr_E^{DF}

Let us define $\mathcal{Y} = \min\{\gamma_S L_{SR}^{-\alpha} N, \gamma_R l^{-\alpha} \Theta\}$. The CDF and PDF of \mathcal{Y} can be, respectively, calculated as

$$F_{\mathcal{Y}}(y) = 1 - \exp\left\{-\frac{y}{\gamma_R l^{-\alpha}}\right\} \mathbb{1}(y < \gamma_S L_{SR}^{-\alpha} N). \quad (76)$$

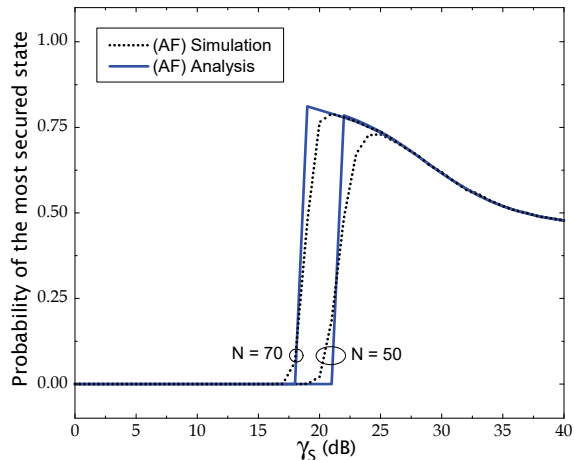


Fig. 9. $\mathbb{P}\{\mathcal{A}\}^{AF}$ versus γ_S . Parameters: $N = \{50, 70\}$, $\lambda = 0.25$, $R_\Psi = 1$, $L_{SR} = 4$, $L_{RD} = 1.5$, $\alpha = 2.5$, $\mu = 16.02$ dB, $\eta = 20$ dB, $\gamma_R = 10$ dB.

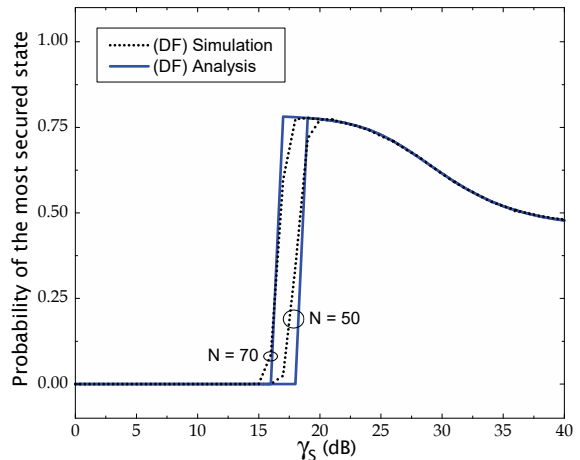


Fig. 10. $\mathbb{P}\{\mathcal{A}\}^{DF}$ versus γ_S . Parameters: $N = \{50, 70\}$, $\lambda = 0.25$, $R_\Psi = 1$, $L_{SR} = 4$, $L_{RD} = 1.5$, $\alpha = 2.5$, $\mu = 16.02$ dB, $\eta = 20$ dB, $\gamma_R = 10$ dB.

and

$$f_Y(y) = \frac{1}{\gamma_R l^{-\alpha}} \exp\left\{-\frac{y}{\gamma_R l^{-\alpha}}\right\} + \exp\left\{-\frac{\gamma_S L_{SR}^{-\alpha} N}{\gamma_R l^{-\alpha}}\right\} \delta(y - \gamma_S L_{SR}^{-\alpha} N) \quad (77)$$

for $y \leq \gamma_S L_{SR}^{-\alpha} N$, where $\delta(y - \gamma_S L_{SR}^{-\alpha} N)$ is a Dirac delta function in y .

Now we can rewrite snr_E^{DF} in (37) as $\text{snr}_E^{AF} = \gamma_S l_{SE}^{-\alpha} |h_{SE}|^2 + \mathcal{Y}$. The CDF of snr_E^{DF} is given by

$$F_{\text{snr}_E^{DF}}(\mu) = \int_0^{\mu_m} F_{|h_{SE}|^2}\left(\frac{\mu - y}{\gamma_S l_{SE}^{-\alpha}}\right) f_Y(y) dy. \quad (78)$$

After some manipulations, (78) is expressed in the form of (44).

C. Proof of Proposition 3

First, we note that both snr_E and SOP_μ are functions of γ_S . To emphasize this, we rewrite snr_E and SOP_μ as $\text{snr}_E(\gamma_S)$ and $\text{SOP}_\mu(\gamma_S)$, respectively. It is straightforward to show $\text{snr}_E(p_2) - \text{snr}_E(p_1) \geq 0$ for $p_2 > p_1$, thus $\text{snr}_E(\gamma_S)$ is an increasing function of γ_S . For $p_2 > p_1$, we have

$$\begin{aligned} & \mathbb{P}\{\text{snr}_E(p_2) < \mu|\Psi\} < \mathbb{P}\{\text{snr}_E(p_1) < \mu|\Psi\} \\ \Rightarrow & 1 - \underbrace{\mathbb{E}_\Psi \left\{ \prod_{Ei \in \Psi} \mathbb{P}\{\text{snr}_E(p_2) < \mu|\Psi\} \right\}}_{\text{SOP}_\mu(p_2)} \\ & > 1 - \underbrace{\mathbb{E}_\Psi \left\{ \prod_{Ei \in \Psi} \mathbb{P}\{\text{snr}_E(p_1) < \mu|\Psi\} \right\}}_{\text{SOP}_\mu(p_1)} \end{aligned} \quad (79)$$

which demonstrates that $\text{SOP}_\mu(\gamma_S)$ increases with γ_S . Moreover, $\lim_{\gamma_S \rightarrow \infty} \text{SOP}_\mu = 1 - \exp\{-\pi\lambda R_\Psi^2\}$ as calculated in (54) and (57) for each considered case, thus this limit value is also the upper bound of SOP_μ at high γ_S .

REFERENCES

- [1] L. J. Rodriguez, N. H. Tran, T. Q. Duong, T. Le-Ngoc, M. Elkashlan, and S. Shetty, "Physical layer security in wireless cooperative relay networks: State of the art and beyond," *IEEE Commun. Mag.*, vol. 53, no. 12, pp. 32–39, Dec. 2015.
- [2] F. Rusek, D. Persson, B. K. Lau, E. G. Larsson, T. L. Marzetta, O. Edfors, and F. Tufvesson, "Scaling up MIMO: Opportunities and challenges with very large arrays," *IEEE Sig. Proc. Mag.*, vol. 20, no. 1, pp. 40–60, Jan. 2013.
- [3] X. Chen, J. Chen, and T. Liu, "Secure transmission in wireless powered massive MIMO relaying systems: Performance analysis and optimization," *IEEE Trans. Veh. Technol.*, vol. 64, no. 10, pp. 8025–8035, Oct. 2016.
- [4] X. Chen, L. Lei, H. Zhang, and C. Yuen, "Large-scale MIMO relaying techniques for physical layer security: AF or DF?" *IEEE Trans. Wireless Commun.*, vol. 14, no. 9, pp. 5135–5146, Sep. 2015.
- [5] G. Amarasuriya, R. F. Schaefer, and H. V. Poor, "Secure communication in massive MIMO relay networks," in *Proc. 17th IEEE Int. Work. Sig. Process. Adv. Wirel. Commun. (SPAWC)*, Edinburgh, UK, Jul. 2016, pp. 1–5.
- [6] C. Zhang, J. Ge, J. Li, F. Gong, and H. Ding, "Complexity-aware relay selection for 5G large-scale secure two-way relay systems," *IEEE Trans. Veh. Tech.*, 2016, to appear.
- [7] J. Chen, X. Chen, W. H. Gerstacker, and D. W. K. Ng, "Resource allocation for a massive MIMO relay aided secure communication," *IEEE Trans. Info. Foren. Sec.*, vol. 11, no. 8, pp. 1700–1711, Aug. 2016.
- [8] T. M. Hoang, T. Q. Duong, H. A. Suraweera, C. Tellambura, and H. V. Poor, "Cooperative beamforming and user selection for improving the security of relay-aided systems," *IEEE Trans. Commun.*, vol. 63, no. 12, pp. 5039–5051, Dec. 2015.
- [9] J. Zhu and W. Xu, "Securing massive MIMO via power scaling," *IEEE Commun. Lett.*, vol. 20, no. 5, pp. 1014–1017, May 2016.
- [10] Y. Wu, R. Schober, D. W. K. Ng, C. Xiao, and G. Caire, "Secure massive MIMO transmission with an active eavesdropper," *IEEE Trans. Info. Theo.*, vol. 62, no. 7, pp. 3880–3900, Jul. 2016.
- [11] N. W. R. S. J. Zhu, D. W. K. Ng and V. K. Bhargava, "Analysis and design of secure massive MIMO systems in the presence of hardware impairments," *IEEE Trans. Wirel. Commun.*, vol. 16, no. 3, pp. 2001–2016, Mar. 2017.
- [12] D. Kapetanovic, G. Zheng, and F. Rusek, "Physical layer security for massive MIMO: An overview on passive eavesdropping and active attacks," *IEEE Commun. Mag.*, vol. 53, no. 6, pp. 21–27, Jun. 2015.
- [13] C. Wang and H.-M. Wang, "Physical layer security in millimeter wave cellular networks," *IEEE Trans. Wirel. Commun.*, vol. 15, no. 8, pp. 5569–5585, Aug. 2016.
- [14] H.-M. Wang, C. Wang, T.-X. Zheng, and T. Q. S. Quek, "Impact of artificial noise on cellular networks: A stochastic geometry approach," *IEEE Trans. Wireless Commun.*, 2016, accepted for publication.
- [15] S. H. Chae, W. Choi, J. H. Lee, and T. Q. S. Quek, "Enhanced secrecy in stochastic wireless networks: Artificial noise with secrecy protected

zone," *IEEE Trans. Inf. Fore. Secu.*, vol. 9, no. 10, pp. 1617–1628, Oct. 2014.

- [16] J. F. C. Kingman, *Poisson Processes*. Oxford University Press, 1993.
- [17] S. N. Chiu, D. Stoyan, W. S. Kendall, and J. Mecke, *Stochastic Geometry and its Applications*, 3rd ed. UK: Wiley, 2013.
- [18] H. ElSawy, E. Hossain, and M. Haenggi, "Stochastic geometry for modeling, analysis, and design of multi-tier and cognitive cellular wireless networks: A survey," *IEEE Commun. Sur. Tut.*, vol. 15, no. 3, pp. 996–1019, Jun. 2013.
- [19] T. Q. Duong, T. M. Hoang, C. Kundu, M. ElKashlan, and A. Nallanathan, "Optimal power allocation for multiuser secure communication in cooperative relaying networks," *IEEE Wireless Commun. Lett.*, vol. 5, no. 5, pp. 516–519, Oct. 2016.
- [20] J. Wang, J. Lee, F. Wang, and T. Q. S. Quek, "Jamming-aided secure communication in massive MIMO Rician channels," *IEEE Trans. Wireless Commun.*, vol. 14, no. 12, pp. 6854–6868, Dec. 2015.
- [21] S. M. A.-Abarghouy, M. N.-Kenari, B. Maham, and M. Hejazi, "Integer forcing-and-forward transceiver design for MIMO multipair two-way relaying," *IEEE Trans. Veh. Tech.*, vol. 65, no. 11, pp. 8865–8877, Nov. 2016.
- [22] S. Y. Seidel, T. S. Rappaport, S. Jain, M. L. Lord, and R. Singh, "Path loss, scattering, and multipath delay statistics in four European cities for digital cellular and microcellular radiotelephone," *IEEE Trans. Veh. Technol.*, vol. 40, no. 4, pp. 721–730, Nov. 1991.
- [23] M. J. Feuerstein, K. L. Blackard, T. S. Rappaport, S. Y. Seidel, and H. H. Xia, "Path loss, delay spread, and outage models as functions of antenna height for microcellular system design," *IEEE Trans. Veh. Technol.*, vol. 43, no. 3, pp. 487–498, Aug. 1994.
- [24] B. Sklar, "Rayleigh fading channels in mobile digital communication systems - Part I: Characterization," *IEEE Communications Magazine*, vol. 35, no. 2, pp. 136–146, Sep. 1997.
- [25] L. Dong, Z. Han, A. P. Petropulu, and H. V. Poor, "Improving wireless physical layer security via cooperating relays," *IEEE Trans. Sig. Process.*, vol. 58, no. 3, pp. 1875–1888, Mar. 2010.
- [26] H. Shin and J. B. Song, "MRC analysis of cooperative diversity with fixed-gain relays in Nakagami-m fading channels," *IEEE Trans. Wirel. Commun.*, vol. 7, no. 6, pp. 2069–2074, June 2008.
- [27] C. D. Meyer, *Matrix Analysis and Applied Linear Algebra*. USA: SIAM, 2000.
- [28] R. E. Prieto, "A general solution to the maximization of the multidimensional generalized Rayleigh quotient used in linear discriminant analysis for signal classification," in *Proc. IEEE Int. Conf. Acou. Spee. Sig. Proc. (ICASSP)*, Hong Kong, Apr. 2003, pp. 157–160.
- [29] J. Lee, H. Wang, J. G. Andrews, and D. Hong, "Outage probability of cognitive relay networks with interference constraints," *IEEE Trans. Wirel. Commun.*, vol. 10, no. 2, pp. 390–395, Feb. 2011.
- [30] J. Hoydis, S. T. Brink, and M. Debbah, "Massive MIMO in the UL/DL of cellular networks: How many antennas do we need?" *IEEE J. Sel. Areas Commun.*, vol. 31, no. 2, pp. 160–171, Feb. 2013.
- [31] H. A. Suraweera, H. Q. Ngo, T. Q. Duong, C. Yuen, and E. G. Larsson, "Multi-pair amplify-and-forward relaying with very large antenna arrays," in *Proc. IEEE Int. Conf. Comm. (ICC)*, Budapest, Hungary, Jun. 2013, pp. 4635–4640.
- [32] J. Hu, W. Yang, N. Yang, X. Zhou, and Y. Cai, "On-off-based secure transmission design with outdated channel state information," *IEEE Trans. Veh. Technol.*, vol. 65, no. 8, pp. 6075–6088, Aug. 2016.



Tiep M. Hoang (S'17) was born in Daklak, Vietnam, in 1989. He received the B.S. degree in Electronics and Electrical Engineering from HCMC University of Technology, Vietnam, in 2012. He received the M.S. degree in Electronics and Radio Engineering from Kyung Hee University, Gyeonggi-do, South Korea, in 2014. During 2015, he worked as a Research Assistant at Duy Tan University, Danang, Vietnam. He is currently a Ph.D. student with the School of Electronics, Electrical Engineering and Computer Science, The Queen's University

of Belfast, The United Kingdom. His current research interests include wireless security, massive MIMO and stochastic geometry.



Trung Q. Duong (S'05, M'12, SM'13) received his Ph.D. degree in Telecommunications Systems from Blekinge Institute of Technology (BTH), Sweden in 2012. Since 2013, he has joined Queen's University Belfast, UK as a Lecturer (Assistant Professor). His current research interests include small-cell networks, ultra-dense networks, physical layer security, energy-harvesting communications, massive MIMO. He is the author or co-author of more than 250 technical papers published in scientific journals (140 articles) and presented at international conferences

(120 papers).

Dr. Duong currently serves as an Editor for the IEEE TRANSACTIONS ON WIRELESS COMMUNICATIONS, IEEE TRANSACTIONS ON COMMUNICATIONS, IET COMMUNICATIONS, and a Senior Editor for IEEE COMMUNICATIONS LETTERS. He was awarded the Best Paper Award at the IEEE Vehicular Technology Conference (VTC-Spring) in 2013, IEEE International Conference on Communications (ICC) 2014, and IEEE Global Communications Conference (GLOBECOM) 2016. He is the recipient of prestigious Royal Academy of Engineering Research Fellowship (2016-2021).



Hoang Duong Tuan received the Diploma (Hons.) and Ph.D. degrees in applied mathematics from Odessa State University, Ukraine, in 1987 and 1991, respectively. He spent nine academic years in Japan as an Assistant Professor in the Department of Electronic-Mechanical Engineering, Nagoya University, from 1994 to 1999, and then as an Associate Professor in the Department of Electrical and Computer Engineering, Toyota Technological Institute, Nagoya, from 1999 to 2003. He was a Professor with the School of Electrical Engineering and Telecommunications, University of New South Wales, from 2003 to 2011. He is currently a Professor with the Faculty of Engineering and Information Technology, University of Technology Sydney. He has been involved in research with the areas of optimization, control, signal processing, wireless communication, and biomedical engineering for more than 20 years.



H. Vincent Poor (S'72, M'77, SM'82, F'87) received the Ph.D. degree in EECS from Princeton University in 1977. From 1977 until 1990, he was on the faculty of the University of Illinois at Urbana-Champaign. Since 1990 he has been on the faculty at Princeton, where he is currently the Michael Henry Strater University Professor of Electrical Engineering. During 2006 to 2016, he served as Dean of Princeton's School of Engineering and Applied Science. His research interests are in the areas of information theory and signal processing, and their applications in wireless networks and related fields such as smart grid and social networks. Among his publications in these areas is the book *Information Theoretic Security and Privacy of Information Systems* (Cambridge University Press, 2017).

Dr. Poor is a member of the National Academy of Engineering, the National Academy of Sciences, and is a foreign member of the Royal Society. He is also a fellow of the American Academy of Arts and Sciences, the National Academy of Inventors, and other national and international academies. He received the Marconi and Armstrong Awards of the IEEE Communications Society in 2007 and 2009, respectively. Recent recognition of his work includes the 2016 John Fritz Medal, the 2017 IEEE Alexander Graham Bell Medal, Honorary Professorships at Peking University and Tsinghua University, both conferred in 2016, and a D.Sc. *honoris causa* from Syracuse University awarded in 2017.